ELSEVIER

Journal of Chromatography A, 965 (2002) 315–356

JOURNAL OF CHROMATOGRAPHY A

www.elsevier.com/locate/chroma

Review

Practice and theory of enantioselective complexation gas chromatography

Volker Schurig*

University of Tübingen, Institute of Organic Chemistry, Auf der Morgenstelle 18, D-72076 Tübingen, Germany

Abstract

The practice and theory of enantioselective complexation GC is comprehensively reviewed for the first time. A multitude of racemic oxygen-, nitrogen- and sulfur-containing selectands can be separated without prior derivatization into enantiomers by complexation GC on optically active metal(II) *bis*[3-(perfluoroacyl)-(1*R*)-camphorate] selectors. Peak inversion is obtained when the selectors with opposite configuration are employed. Applications pertain to chiral analysis in asymmetric synthesis, enzymatic reactions, pheromone and flavour chemistry. Although the use of enantioselective complexation GC has diminished recently with the advent of modified cyclodextrins in enantioselective GC, the inherent principles of enantiorecognition together with other enantioselective phenomena can be elucidated easily by complexation GC. Using the concept of the retention-increment R' which allows the distinction between non-enantioselective and enantioselective contributions to retention, concise thermodynamic parameters of enantioselectivity $-\Delta_{D,L}(\Delta G)$ are accessible. The enantiomerization of configurationally labile enantiomers can be investigated and quantified by complexation GC. Four distinct enantioselective processes and four different coalescence phenomena have been discerned in complexation GC.

Keywords: Reviews; Enantiomeric separation; Isoenantioselective temperature; Enantioselective complexation; Enantioselectivity; Enantiorecognition; Chiral non-racemic metal β-diketonates

Contents

*Tel.: +49-707-129-6257; fax: +49-707-129-5538.
E-mail address: volker.schurig@uni-tuebingen.de (V. Schurig).

0021-9673/02/$ – see front matter
PII: S0021-9673(01)01500-X

1. Practice of complexation GC

1.1. Introduction

The resolution of racemic *N*-trifluoroacetyl amino acid alkyl esters on glass capillary columns coated with chiral L-*N*-trifluoroacetyl isoleucine lauryl ester by Gil-Av, Feibush and Charles-Sigler in 1966 [1] represented the first instance of the direct separation of enantiomers by GC. The propensity for hydrogen-bonding and the remote resemblance of the solute–solvent pair to a peptide–enzyme complex intuitively guided the choice of the enantioselective system. Subsequently, Gil-Av and Schurig realized that essentially abiotic *selector–selectand*[1] systems, e.g. those displaying metal–organic coordination, should be prone to enantiorecognition in *complexation gas chromatography*[2]. Thus in 1970 research was initiated aimed at the gas-chromatographic separation of the enantiomers of a racemic olefin on a chiral metal complex – a profound academic challenge but with little practical interest at that time. The π-complexation ability of silver(I) ions toward olefins was utilized for selective alkene separations by *argentation chromatography* at the beginning of the 1960s [4–7] and was consequently extended by Gil-Av and Schurig to the quantitative gas-chromatographic study of olefin–rhodium(I) coordination equilibria [8–11] (the state of the art was reviewed recently [12]). The use of chiral transition metal complexes as selectors containing optically active phosphines and phosphites appeared obvious but proved unsuccessful despite their subsequent versatility in transition-metal-mediated asymmetric catalysis. Subsequently, Feibush suggested the use of a chiral β-diketonate anion obtained from natural (+)-camphor by trifluoroacetylation, i.e. 3-(trifluoroacetyl)-(1*R*)-camphorate, as chiral ligand for transition metal ions – previously utilized for lanthanide metal ions [13]. A key step consisted of the synthesis of dicarbonyl–rhodium(I) 3-(trifluoroacetyl)-(1*R*)-camphorate **1** (cf. Scheme 1) [14].

[1] This term was coined by Mikeš in 1975 [2] in analogy to Ashby's terms operator–operand.

[2] This term was later introduced by Schurig in 1976 [3].

1.2. The separation of a racemic olefin into enantiomers by complexation GC

After many unsuccessful trials, the separation of a racemic olefin into enantiomers by complexation GC on (1*R*)-**1** was reported in 1977 [15,16]. Thus when racemic 3-methylcyclopentene was gas-chromatographed on a 200 m×0.5 mm I.D. stainless steel capillary column coated with pure squalane its retention relative to the reference compound

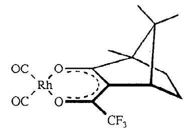

1

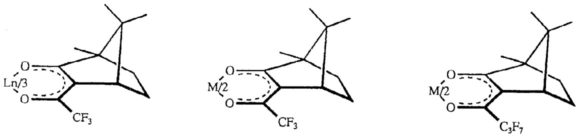

2 : Ln = Eu(III)

3a : M = Ni(II)
3b : M = Co(II)
3c : M = Mn(II)

4a : M = Ni(II)
4b : M = Co(II)
4c : M = Mn(II)

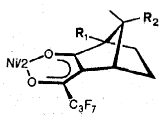

5a : R_2 = $-CH_3$; R_1 = $-CH{=}CH_2$
5b : R_2 = $-CH_3$; R_1 = $-CH_2CH_3$
5c : R_2 = $-CH_3$; R_1 = $-CH{=}CH{-}CH_3$
5d : R_2 = $-CH_3$; R_1 = $-CH{=}CH{-}CH(CH_3)_2$

5e : R_1 = $-CH_3$; R_2 = $-CH{=}CH_2$
5f : R_1 = $-CH_3$; R_2 = $-CH_2CH_3$

Scheme 1. Structures of metal 3-perfluoroacyl-camphorates.

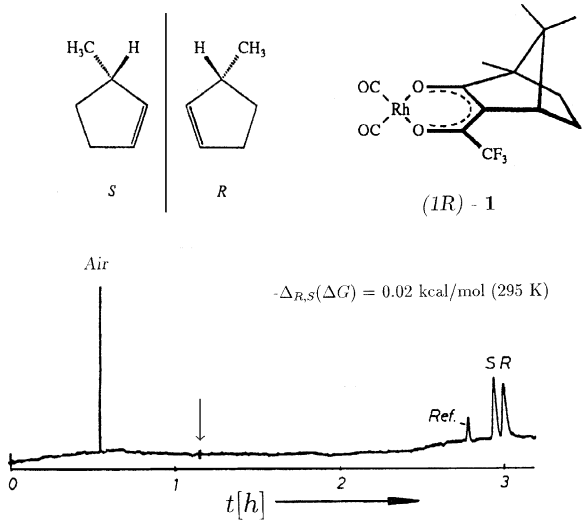

Fig. 1. Separation of the enantiomers of 3-methylcyclopentene by complexation GC on 0.04 *m* (1*R*)-**1** in squalane at 22°C, $\alpha = 1.025$ (column: 200 m×0.5 mm I.D. stainless steel; carrier gas: dinitrogen). Inert reference compound: methylcyclohexane. Arrow: elution position of the olefin on pure squalane [14].

methylcyclohexane was $r^{\circ} = 0.26$ at 22 °C (cf. arrow in Fig. 1). When the same olefin was injected on a column coated with a solution of 0.04 *m* (molality) of **1** in squalane the enantiomers were strongly retarded and eluted after the reference compound methylcyclohexane with different retentions (r_S = 1.069 and r_R = 1.097) at 22 °C [15] (cf. Fig. 1).

The difference of the Gibbs energy (free enthalpy) of the enantioselective complexation of 3-methylcyclopentene with **1** was as small as $-\Delta_{R,S}(\Delta G) = RT \ln(K_R/K_S) = 0.02$ kcal/mol (295 K) calculated from $K_R/K_S = 1.035$ (cf. Section 2.2.). It is noted that this small Gibbs energy difference corresponded to a separation factor $\alpha = 1.026$, sufficient for a quantitative separation of the enantiomers on the high-resolution capillary column used. Two decisive control experiments were performed to verify the first separation of the enantiomers by complexation GC and excluding any artifact: (i) the racemic selector (1*R*/1*S*)-**1** was synthesized and employed as *optically inactive* stationary phase; as expected, only one peak was observed for the enantiomers (*peak coalescence of the second kind*, cf. Section 2.11) [15] and (ii) the selector (1*S*)-**1** was synthesized from unnatural (−)-camphor and was used as *chiral stationary phase with opposite configuration*; as expected, reversal of the order of elution was observed for a sample of the olefin enriched in the (*R*)-enantiomer (*peak inversion of the first kind*) [16]. The observation of peak coalescence and peak inversion represented a unequivocal evidence for the separation of a racemic selectand on a chiral selector used in both enantiomeric forms and as a racemic mixture in three different trials. During the course of these control experiments an unexpected discovery was made which was unprecedented in chiral solid state chemistry and which was of interest in its own right. Whereas both enantiomers of (1*R*)- and (1*S*)-**1** form yellow crystals, racemic (1*R*/1*S*)-**1** crystallizes as a deeply red–green dichroic solid (cf. Fig. 2) [17]. This phenomenon was called *chirodichroism*. It

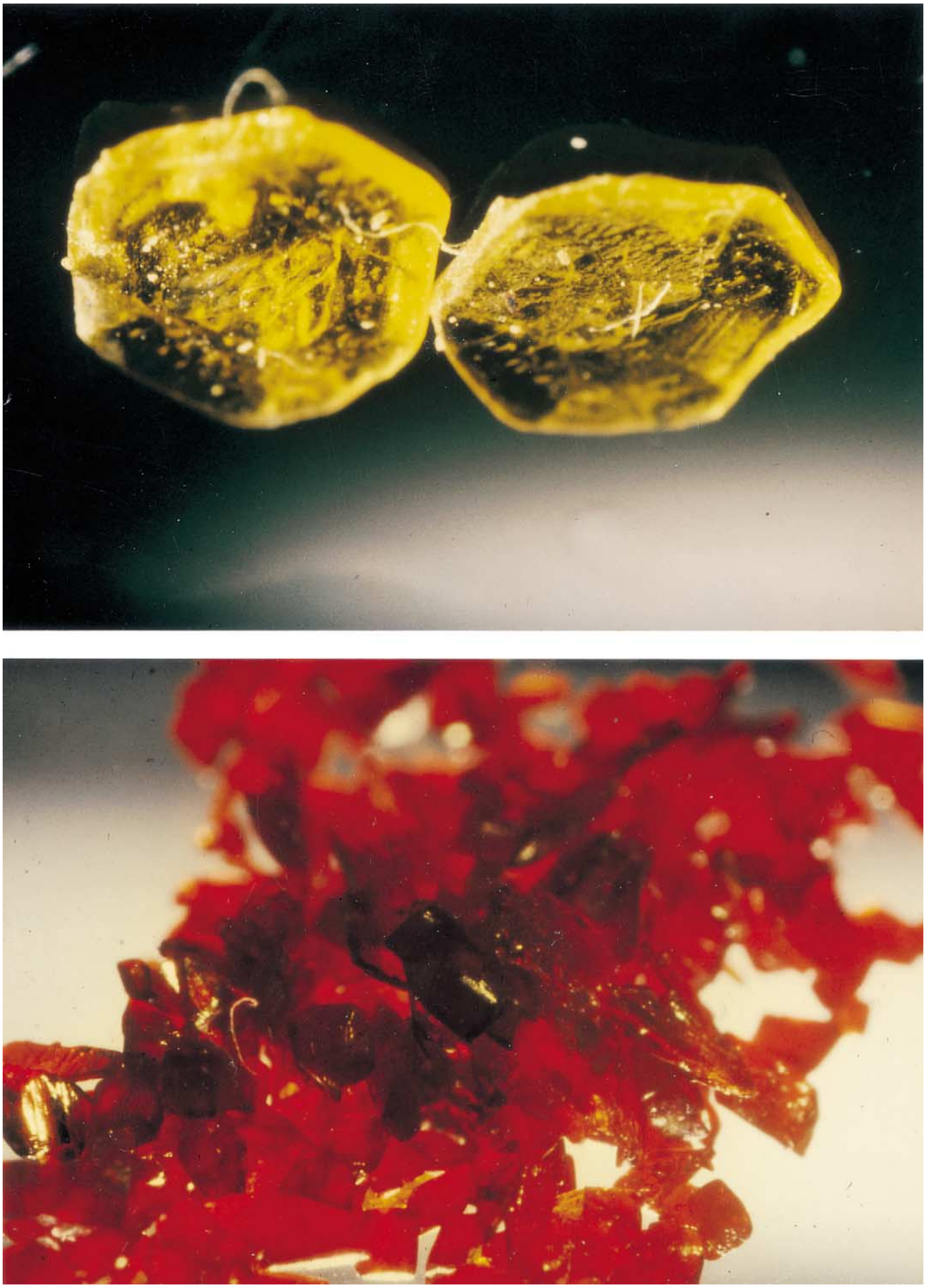

Fig. 2. Chirodichroism in the solid state of dicarbonyl–rhodium(I) 3-(trifluoroacetyl)-(1*R*)-camphorate. Top: crystals of the pure enantiomer (1*R*)-**1**. Bottom: crystals of the racemate (1*R*/1*S*)-**1** [17].

underlines vividly the inherent differences between pure enantiomers and the racemic mixture in the solid state[3] [17].

Although the scope of the separation of racemic olefins by complexation GC on **1** was limited [18], the important applications in the area of chiral analysis [19] were immediately apparent. Thus the specific rotation of enantiomerically impure (by GC evidence) 3-methylcyclopentene was extrapolated to α_{max} and corrected to more than double that reported in literature [16]. Based on the new value, chiroptical calculations and the enantiomeric excess *ee* obtained via asymmetric borane chemistry had to be revised for this chiral olefin [16]. Furthermore, a small degree of kinetic resolution of 3-methylcyclopentene during enantioselective rhodium(I)–phosphane-catalyzed hydrogenation was detected (cf. Fig. 5 in Ref. [19]).

1.3. Extension of the scope of enantioselective complexation gas chromatography to oxygen-, nitrogen- and sulfur-containing racemic compounds – separation of enantiomers on metal(II) bis[α-(perfluoroacyl)-terpeneketonates]

Whereas the scope of enantiomer separation of olefins on dicarbonyl–rhodium(I) 3-(trifluoroacetyl)-(1*R*)-camphorate **1** was limited (cf. Section 1.2), the use of metal(II) *bis*[3-(trifluoroacetyl)-(1*R*)-camphorates] **3** and metal(II) *bis*[3-(heptafluorobutanoyl)-(1*R*)-camphorates] **4** (metal = nickel, cobalt and manganese) as chiral selectors for the separation of the enantiomers of nitrogen-, oxygen- and sulfur-containing selectands soon emerged as a routine method for the gas chromatographic analysis of enantiomers [20–22]. Typical enantiomeric separations are shown in Figs. 3–6. The classes of compounds separated encompass inter alia small cyclic ethers [20], underivatized alcohols and ketones (cyclic [22] and acyclic [23]), alkyl 2-halocarboxylates [24] and acetals [22,25]. Most of these compounds are not amenable to separation by hydrogen-bonding chiral stationary phases (CSPs) [26].

Golding et al. reported the first separation of enantiomers of methyl- and ethyloxirane by packed complexation GC using a 2 m × 2.2 mm I.D. column containing a support which was coated with europium(III) *tris* [3-(trifluoroacetyl)-(1*R*)-camphorate] **2** in squalane [30]. Such a separation was predicted [13,31] in view of the versatility of **2** as a chiral NMR shift reagent. In principle, any volatile chiral selectand containing a complexing function closely juxtaposed to the chiral center should be prone to enantiorecognition by complexation GC on a suitable chiral metal containing selector. The application of high-resolution glass or fused-silica capillary column technology in complexation GC greatly improved the state of the art and squalane was later replaced by dimethylpolysiloxane as unique solvent for the selectors **3–4** [21,32,33]. A very simple procedure consists of the impregnation (doping) of chemically bonded dimethylpolysiloxane fused-silica columns with an *n*-pentane solution of freshly sublimed **4a** by the dynamic coating procedure.

Significantly, the metal selectors are capable of separating one of the smallest classes of chiral compounds namely alkyl-substituted oxiranes, aziridines and thiiranes [20]. The possibility of determining the enantiomeric excess *ee* of chiral oxiranes permitted the study of metal-catalyzed asymmetric oxidations. Thus the first enantioselective epoxidation of aliphatic olefins by a chiral molybdenum–peroxo complex with enantiomeric excesses *ee* up to 40% was described [34] followed by investigations on the kinetic resolution of the oxiranes by the same molybdenum complex in the presence of a chiral diol [35]. These advances are early examples for the well-known systems titanium/tartrate (Katsuki–Sharpless epoxidation) and manganese(II)–salen (Jacobson kinetic resolution) [36]. The refined analytical tool of complexation GC permitted also the investigation of the Cytochrom-P 450-mediated epoxidation of xenobiotic prochiral simple olefins (propene, 1-butene, *trans*-2-butene etc.) [37,38] and kinetic resolution of the oxiranes formed (methyloxirane, ethyloxirane, *trans*-2,3-dimethyloxirane etc.) by epoxide–hydrolase and glutathion-*S*-transferase [39]. For *cis*-2-ethyl-3-

[3] A columnar structure with close metal–metal contacts leading to dichroism is built-up in the red–green racemate whereas only a zig-zag arrangement rather than a metal chain is formed in the single yellow enantiomers.

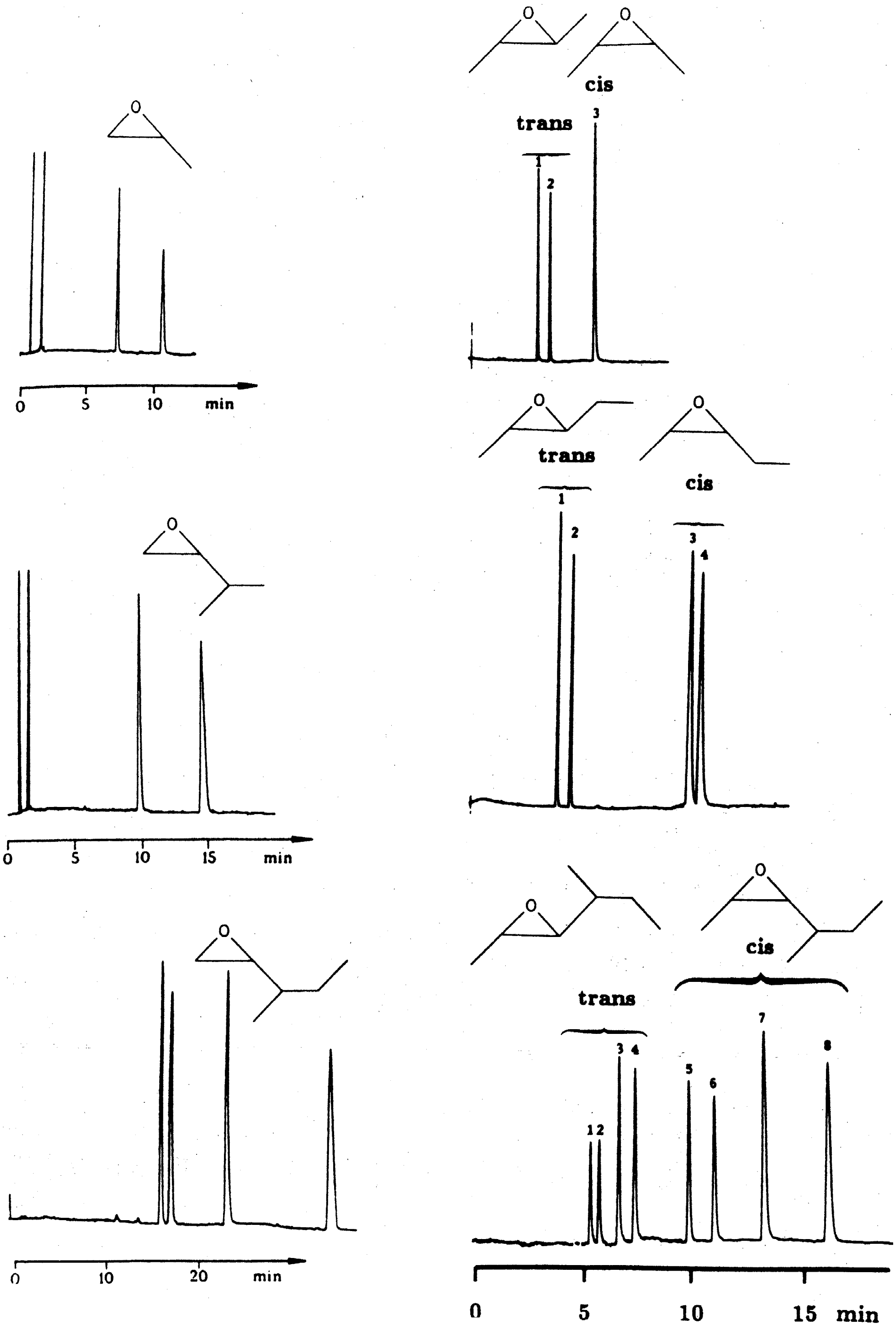

Fig. 3. Separation of the enantiomers of 2-alkyl- and 2,3-dialkyloxiranes by complexation GC. 25 m×0.25 mm I.D. glass capillary column coated with 0.125 *m* nickel(II) *bis*[3-(heptafluorobutanoyl)-10-(ethylidene)-(1*S*)-camphorate] **5c** in OV-101 at 70–90 °C [27,28]. Peak assignment of 2-*sec*-butyl-3-methyloxiranes (by independent synthesis): *trans*: 1: 2*S*,3*S*,1′*S*; 2: 2*R*,3*R*,1′*R*; 3: 2*S*,3*S*,1′*R*; 4: 2*R*,3*R*,1′*S*. *cis*: 5: 2*S*,3*R*,1′*R*; 6: 2*R*,3*S*,1′*S*; 7: 2*S*,3*R*,1′*S*; 8: 2*R*,3*S*,1′*R*.

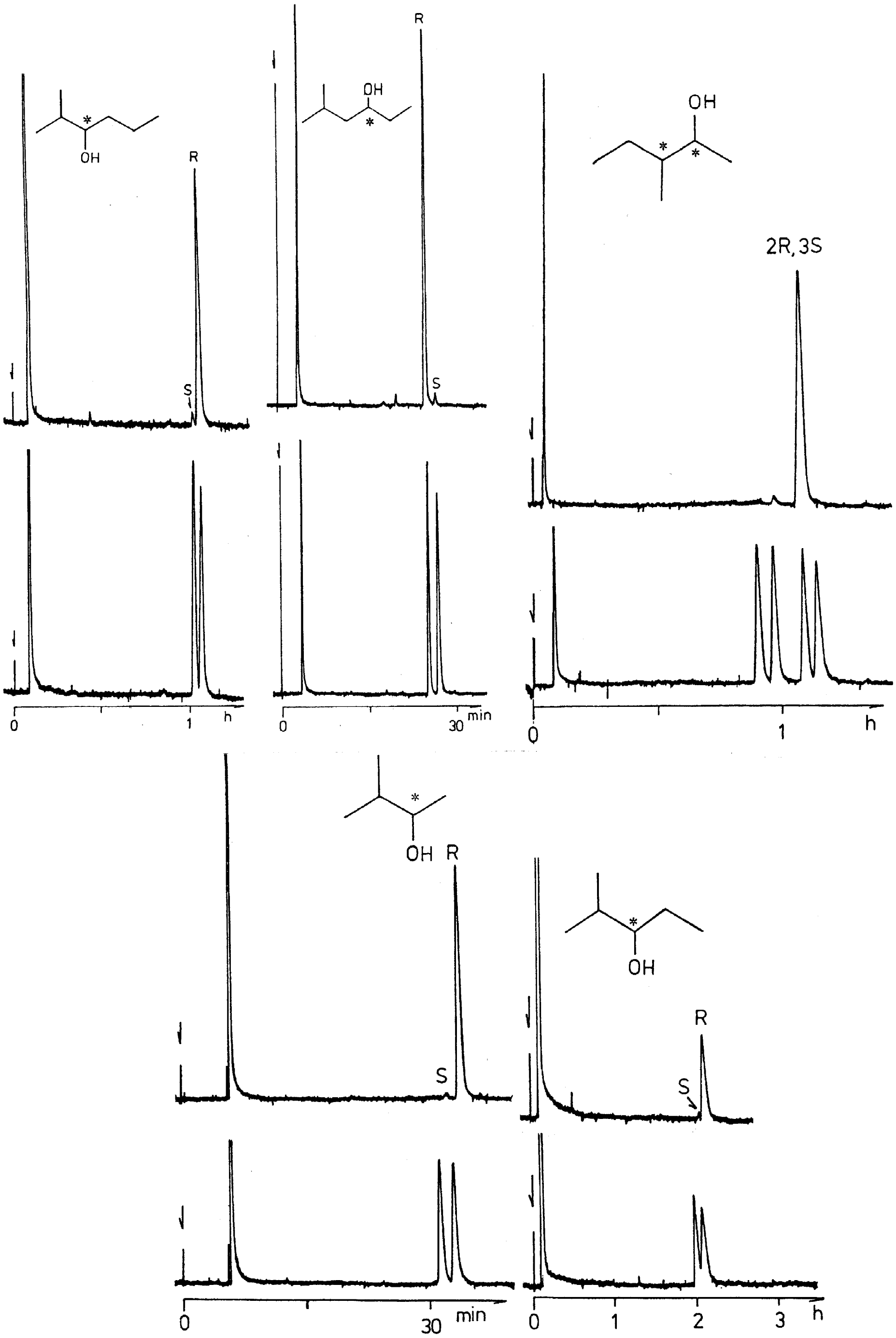

Fig. 4. Separation of the enantiomers of underivatized aliphatic alcohols with concomitant peak assignment. Column: 40 m×0.25 mm I.D. glass capillary coated with 0.1 *m* manganese(II) *bis*[3-(heptafluorobutanoyl)-(1*R*)-camphorate] **4c** in OV 101. Top left: 2-methylhexane-3-ol, 54 °C, 0.5 bar dinitrogen. Top middle: 5-methylhexane-3-ol, 70 °C, 1.0 bar dinitrogen. Top right: 3-methylpentane-2-ol, 55 °C, 0.5 bar dinitrogen. Bottom left: 3-methylbutane-2-ol, 54 °C, 0.6 bar dinitrogen. Bottom right: 2-methylpentane-3-ol, 60 °C, 0.4 bar dinitrogen [23,29].

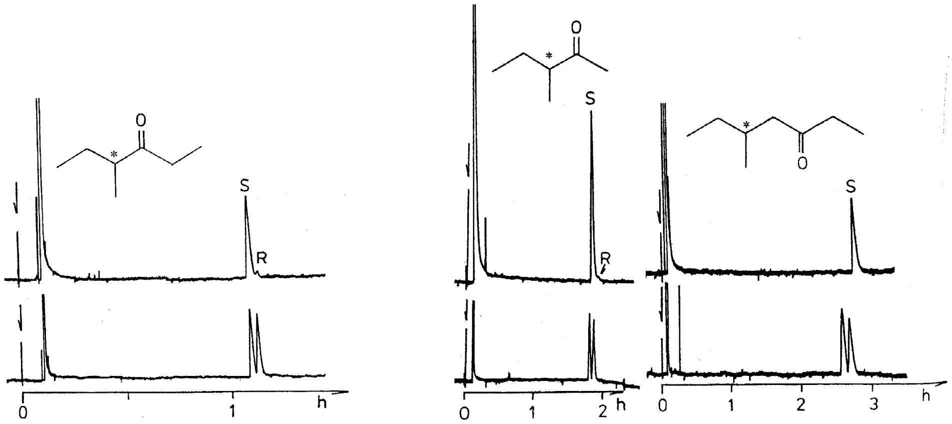

Fig. 5. Separation of the enantiomers of underivatized aliphatic ketones with concomitant peak assignment. Column: 37 m×0.25 mm I.D. coated with 0.125 *m* nickel(II) *bis*[3-(heptafluorobutanoyl)-(1*R*)-camphorate] **4a** in OV 101. Left: 4-methylhexane-3-one, 70 °C and 0.4 bar dinitrogen. Center: 3-methylpentane-2-one, 80 °C and 1.0 bar dinitrogen. Right: 5-methylheptane-3-one, 80 °C and 1.0 bar dinitrogen [23,29].

methyloxirane a complete regio- and enantioselective kinetic resolution with microsomal epoxide-hydrolase was found [40]. Also the evidence of high enantiomeric excesses (*ee*) in the chirality pool synthesis of aliphatic oxiranes from natural amino acids was accomplished by complexation GC [41].

Before the advent of modified cyclodextrins, enantioselective complexation GC represented also a very useful tool for chiral analysis of volatile compounds such as flavours [22,32,33,42,43] and insect pheromones [25,44–47]. In Fig. 7 the determination of the enantiomeric ratio of *endo*-brevicomin isolated from the Mountain pine bark beetle is shown [48]. Surprisingly, the pheromone was neither racemic nor enantiomerically pure.

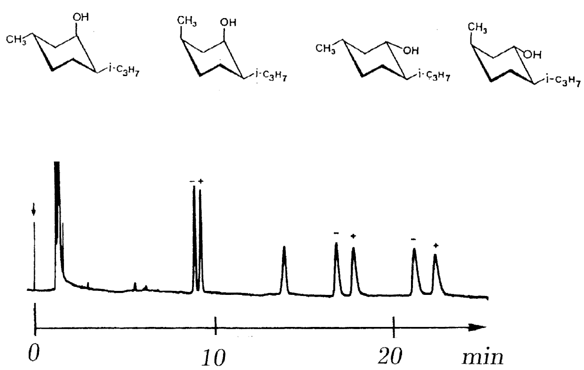

Fig. 6. Diastereomeric and enantiomeric separation of underivatized *p*-3-menthanols. 28 m×0.25 mm I.D. glass capillary column coated with 0.08 *m* nickel(II) *bis*[3-(heptafluorobutanoyl)-(1*R*)-camphorate] **4a** in OV-101 at 116 °C and 1 bar dinitrogen. Only *neoiso*-menthol is not separated into enantiomers [32,33].

1.4. Chirasil-Metal stationary phases for complexation GC

In a pioneering advance, Frank, Nicholson and Bayer linked the valine diamide selector of Gil-Av and Feibush to a polysiloxane-copolymer [50] by total synthesis. The resulting chiral polysiloxane containing valine abbreviated *Chirasil-Val*, commercially available in both enantiomeric forms, combined the enantioselectivity of the amino acid selector with the universal gas-chromatographic properties of polysiloxanes. Other groups used polymer-analogous reactions to obtain related chiral polymeric CSPs [51,52].

The strategy to link the chiral metal-containing selector to a polymeric backbone was also followed in complexation GC. A limiting factor of coordination-type CSPs was the hitherto low temperature range of operation (25–120°C). The thermostability was therefore increased by the preparation of immobilized polymeric CSPs. Chiral polysiloxanes with metal-containing stationary phases, i.e. Chirasil-Metal, **6** and **7**, were obtained by total synthesis (cf. Scheme 2) [53] or, preferentially, by polymer-analo-

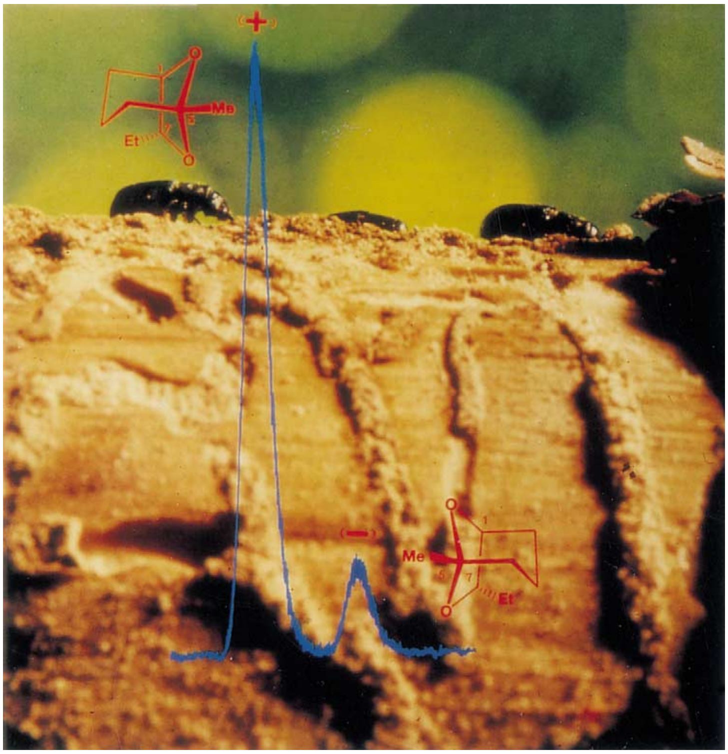

Fig. 7. Complexation GC–MS of the enantiomers of *endo*-brevicomin, $m/e=98$ (configurations inserted in blue) isolated from the mountain bark beetle *Dendroctonus ponderosae* from Oregon, USA. (+):(−)=87.5:12.5% (*ee*=75%) [49].

gous reaction (cf. Scheme 3) [54]. By thermal treatment, Chirasil-Metal stationary phases can be immobilized on the glass or fused-silica surface due to the presence of residual hydro-silane entities in the polymer as the 10-methylene-camphor moiety was linked via hydrosilylation to the polysiloxane backbone. Incidentally, by introducing unsaturation into the camphor moiety, new ligands were obtained for nickel(II). Despite the small changes in structure, the new selectors **5** (cf. Scheme 1) exhibited profound differences in enantioselectivity (cf. Section 2.6).

The fast separation of the enantiomers of 2-methyl-substituted cyclic ethers on thermally immobilized Chirasil-Nickel **7a** is shown in Fig. 8.

Immobilized Chirasil-Nickel **7a** is compatible with highly solvating mobile phases such as supercritical carbon dioxide. Hence, fused-silica capillary columns coated with Chirasil-Nickel **7a** can be utilized in complexation supercritical fluid chromatography (complexation SFC) (cf. Section 1.6.). Chirasil-Europium **7d** can be employed in four different areas: (i) in enantioselective complexation GC, (ii) as enantioselective polymeric NMR shift reagent, (iii) as enantioselective catalyst for a hetero-Diels–Alder reaction [55] and (iv) as coating of quartz microbalances for the determination of VOCs [56].

Chirasil-Metal stationary phases have also been prepared in which the metal centers represent the terminating groups of the polymer [56].

1.5. Separation of enantiomers by complexation supercritical fluid chromatography

Enantioselective complexation GC has never been extended to LC or CE because it was believed that the mobile phase consisting of water or polar modifiers would compete with the selectand for free coordination sites of the metal β-diketonate selectors, thereby blocking the complexation with oxygen-, nitrogen- and sulfur-containing compounds.

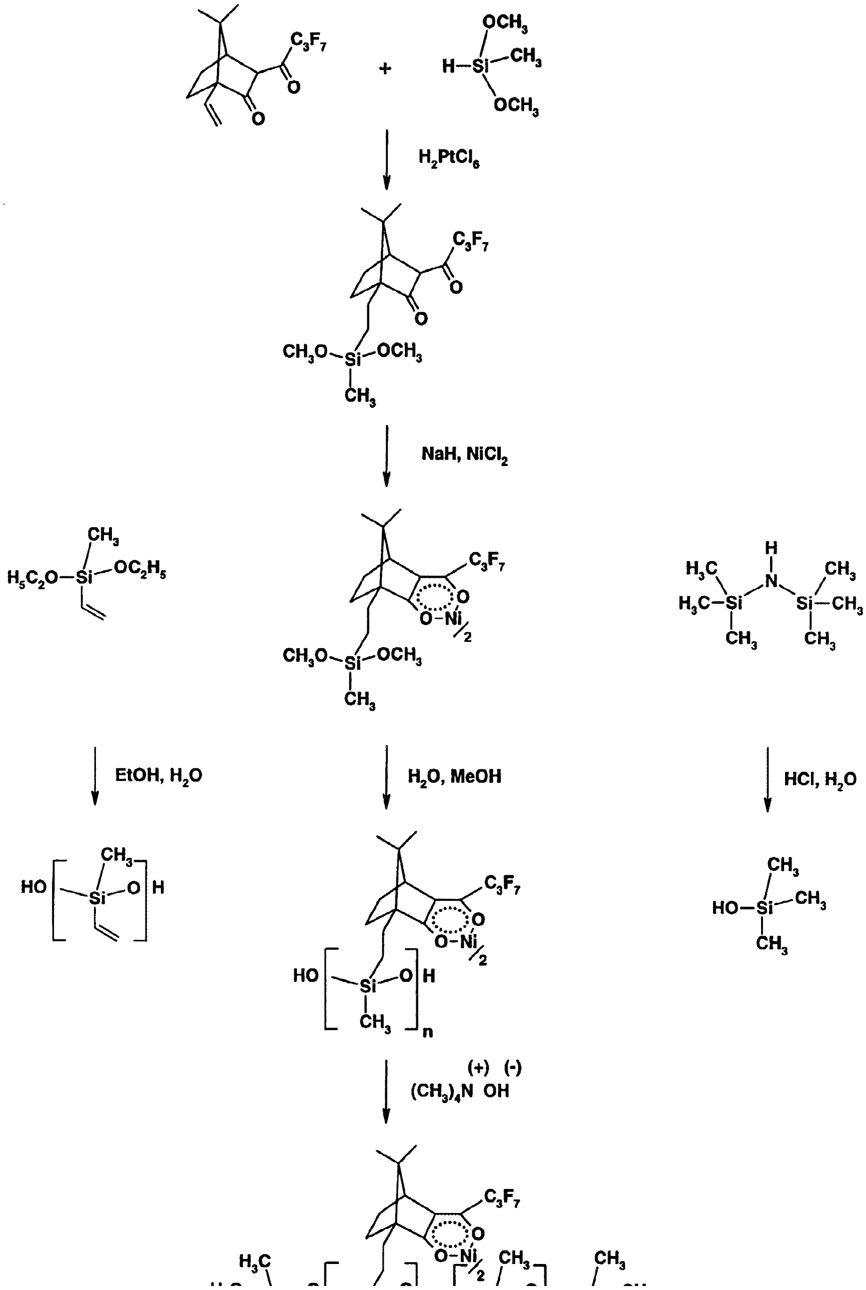

Scheme 2. Total synthesis of the chiral polysiloxane Chirasil-Nickel **6**. The random ratio of methylvinylsiloxane to nickel-containing methylsiloxane monomers in the polymer is ~7:1. The nickel content (by atomic absorption) is 11 mg/g polymer or ~0.2 *m* [53].

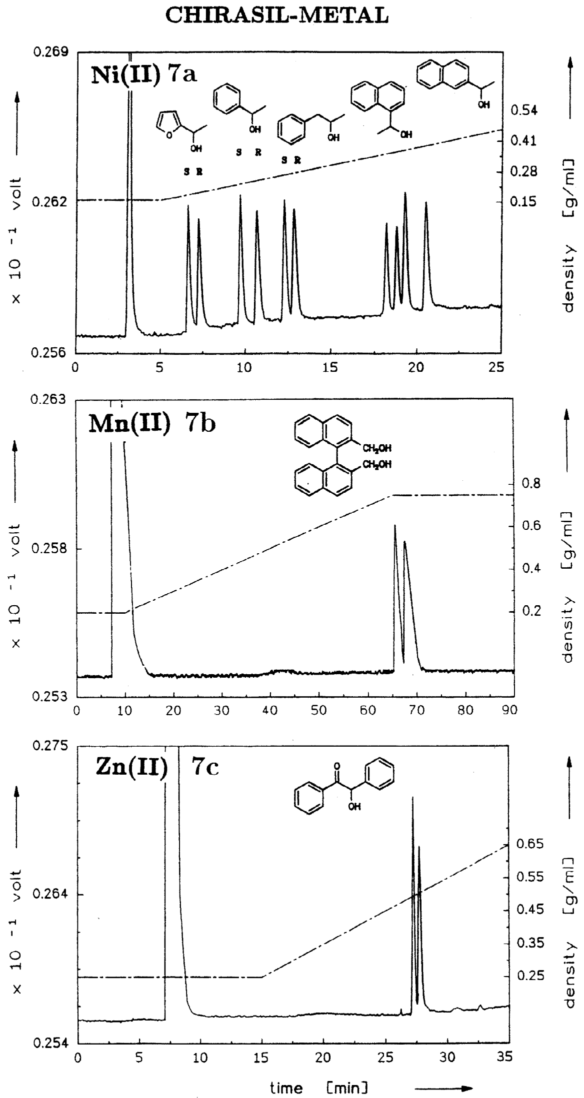

Fig. 9. Separation of enantiomers by complexation SFC on Chirasil-Nickel **7a**. Top: underivatized secondary alcohols. 2 m× 0.05 mm I.D. fused-silica column coated with Chirasil-Nickel **7a** (0.25 μm). CO_2 at 120 °C. Density program as indicated, FID. Center: 2,2′-(dihydroxymethylene)-1,1′-binaphthyl. 4 m×0.05 mm I.D. fused-silica column coated with Chirasil-Manganese **7b** (0.25 μm). CO_2 at 120 °C. Density program as indicated, FID. Bottom: benzoin. 2.5 m×0.05 mm I.D. fused-silica column coated with Chirasil-Zinc **7c** (0.25 μm). CO_2 at 70 °C. Density program as indicated, FID [58].

SFC has been investigated (cf. Fig. 11) [58,59]. Unusual peak broadening phenomena observed in enantioselective complexation SFC are discussed in Section 2.9.

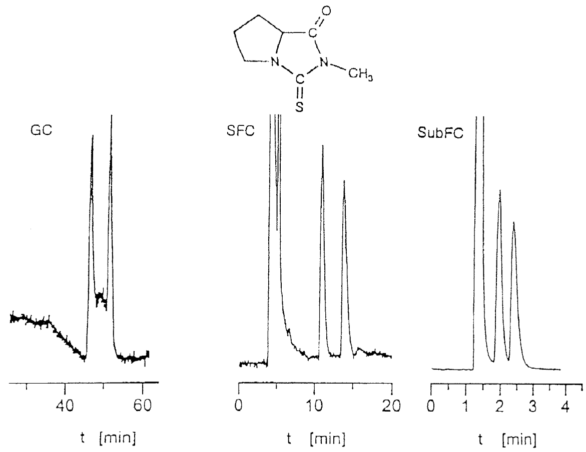

Fig. 10. Separation of the enantiomers of MTH-proline on Chirasil-Nickel **7a**. Left: GC, 19 m×0.25 mm I.D. fused-silica column coated with **7a**, 130 °C, 1 bar helium (plateau formation due to enantiomerization). Center: SFC, 5 m×0.05 mm I.D. fused-silica column coated with **7a**, 60 °C, $\rho=0.55$ g/ml. Right: subFC, 5 m×0.05 mm I.D. fused-silica column coated with **7a** 27°C, $P_i=35$ MPa [59].

1.6. Semipreparative separation of enantiomers by complexation GC

Packed columns containing **2** and **3** in squalane had thoroughly been investigated before the advent of chiral separations [13,31]. Following the report of Golding et al. on the separation of the enantiomers of methyloxirane by complexation GC using a packed column [30] it was obvious that semipreparative separations of enantiomers by complexation GC would be feasible for volatile racemates with large separation factors α. This was confirmed by the semipreparative separation of the enantiomers of 1-chloro-2,2-dimethylaziridine (cf. Fig. 12, top, A) [29,60]. Chiroptical data, the nitrogen inversion barrier and the absolute configuration, leading to the correction of the assignment in the literature, were determined from the isolated invertomers [29,60]. The racemization kinetics of the isolated pure enantiomer of (*S*)-1-chloro-2,2-dimethylaziridine was checked by complexation GC with an analytical column (cf. Fig. 12, top, B).

The semipreparative separation of all four stereoisomers of 2-ethyl-1,6-dioxaspiro[4.4]nonane, chalcogran (A–D, configurations, cf. Scheme 4) on nickel(II) *bis* [5-(heptafluorobutanoyl)-(*S*)-carvonate] **14** is shown in Fig. 12, bottom [22,61].

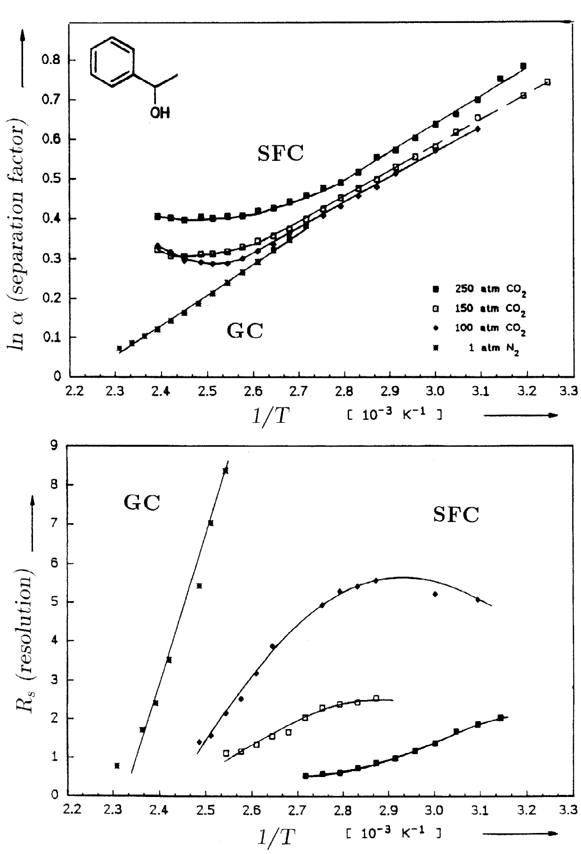

Fig. 11. GC–SFC comparison of separation factors α and resolution R_s as function of temperature for 1-phenylethanol in complexation chromatography at different mobile phase pressures; 2 m×0.05 mm I.D. fused-silica column coated with Chirasil-Nickel **7a** [58].

Unfortunately, the retention times were exceedingly long.

1.7. Isotopic separation of α-deuterated tetrahydrofurans and the elusive separation of protio/deutero-substituted enantiomers

Following an early report on the separation of deuterated ethenes on **1** [3], the quantitative discrimination of isotopomers with a mass difference of one dalton by complexation GC was also found for the separation of α-deuteriated tetrahydrofurans $C_4H^{\alpha}_{4-n}D^{\alpha}_nH^{\beta}_4O$, on cobalt(II)–*bis*[3-(heptafluorobutanoyl)-(1*R*)-camphorate] **3b** in less than 30 min at 70 °C [62] (cf. Fig. 13).

The separation is due to a marked inverse secondary isotope effect $K_D/K_H > 1$. As expected, the inverse isotopic effect rapidly decreases with the distance from the complexing oxygen atom. Thus d_8-tetrahydrofuran and α-d_4-tetrahydrofuran were not separated and attempts to separate ^{18}O–tetrahydrofuran from ^{16}O–tetrahydrofuran by complexation GC have failed thus far.

One of the challenges in separation science is to resolve stereoisomers owing their chirality to isotopically substituted compounds. Thus αα′-d_2-tetrahydrofuran contains two stereogenic centers –OC*(H,D)CH_2– giving rise to the occurrence of three stereoisomers. As seen in Fig. 13 separation of the *meso*/*rac*-diastereomeric pair as well as the *rac*-enantiomeric pair of (2) on the chiral selector (1*R*)-**4b** is not observed. The enantiomers of ‘‘crypto’’-chiral α-d_1-tetrahydrofuran (1) and ααα′-d_3-tetrahydrofuran (3) are also not separated. Further attempts to separate chiral isotopically labeled compound by complexation GC such as d_1-2,2-dimethyl-1-propanol, *cis*-(d_3-methyl)-(h_3-methyl)-oxirane and (d_9-*tert*-butyl)-(h_9-*tert*-butyl)-methylcarbinol and derivatives thereof have failed thus far. Interestingly, the enantiomers of d_1-2,2-dimethyl-1-propanol [63] and of (d_9-*tert*-butyl)-(h_9-*tert*-butyl)-methylcarbinol [64] can be distinguished by proton or deuterium NMR in the presence of chiral lanthanide shift reagents such as europium(III)–*tris*[3-(heptafluorobutanoyl)-(1*R*)-camphorate] (a homologue of **2**). This result provides evidence that isotopic enantiomer discrimination by NMR in chiral solvating agents is the result of a chemical shift anisochrony of diastereotopic nuclei rather than due to a difference of diastereomeric complexation constants K_D/K_L [64].

1.8. Assignment of absolute configurations by complexation GC

The determination of *absolute configurations* of chiral analytes is an important task in enantiomer analysis. Absolute configurations of minute amounts of chiral samples may be determined *directly*, and free of chiroptical evidence, by GC via coinjection of reference compounds with known stereochemistry. Absolute configurations of alkyloxiranes can also be predicted *indirectly*. Thus an empiric *quadrant rule* has been formulated that correlates the absolute configuration with the order of elution of an oxirane on nickel(II) *bis*[3-(trifluoroacetyl)-(1*R*)-campho-

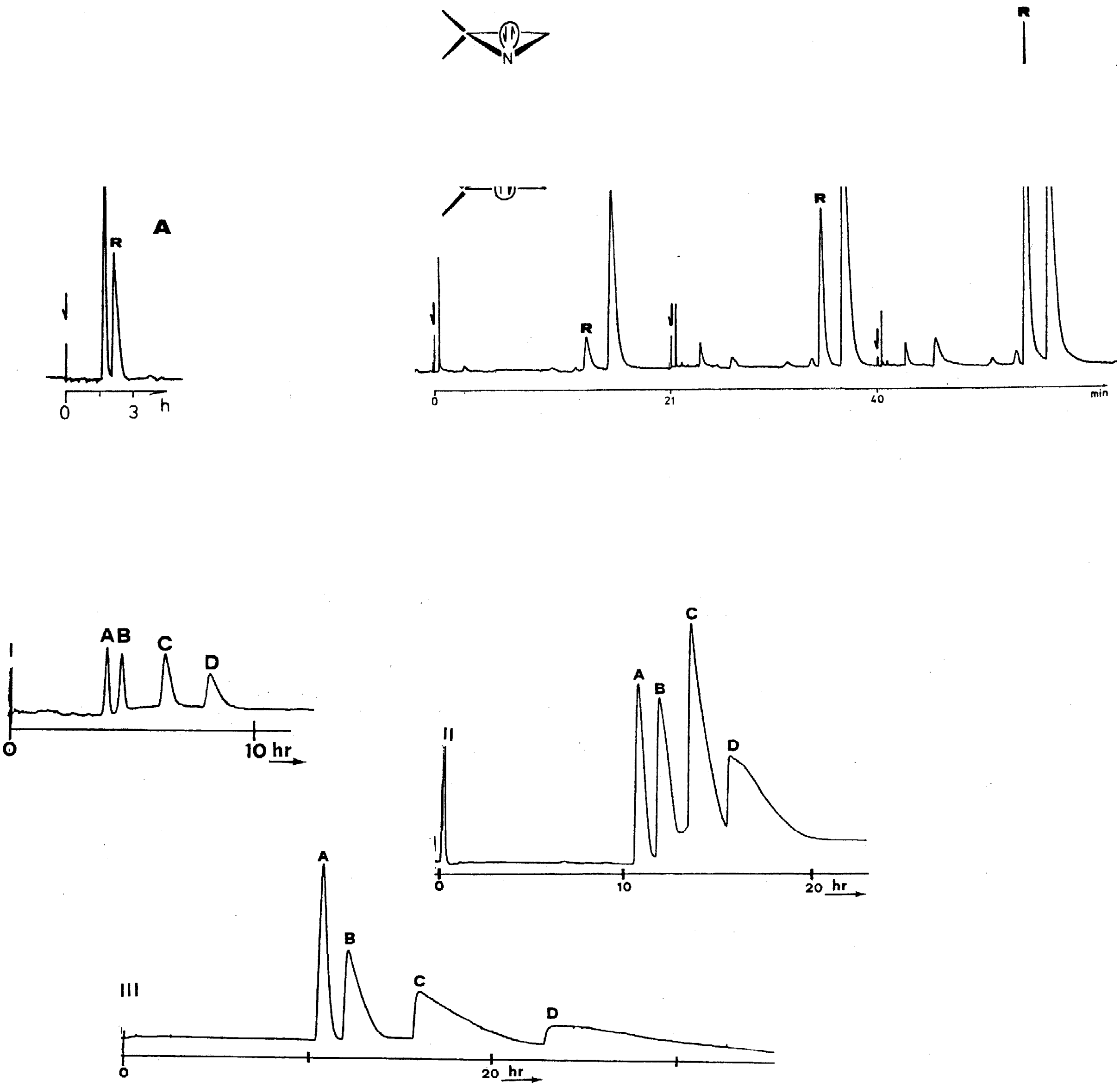

Fig. 12. Semi-preparative separation of enantiomers by complexation GC. Top A: 1-chloro-2,2-dimethylaziridine. 7.5 m×3 mm I.D. stainless steel column filled with 250 mg **3a** and 6.25 g OV 101 impregnated on 43 g Chromosorb (W-AW-DMCS, 60/80 mesh) at ambient temperature and 1.5 bar dinitrogen. Top B: Racemization kinetics of (*S*)-1-chloro-2,2-dimethylaziridine in the gas phase at 82 °C. Analytical GC conditions: 25 m×0.25 mm I.D. glass capillary column coated with 0.125 *m* **12** in OV 101 at 22 °C (the low temperature is used to prevent enantiomerization) and 1 bar dinitrogen. The change of the elution order on the two different selectors **3a** and **12** should be noted [29,60]. Bottom: 2-ethyl-1,6-dioxaspiro[4.4]nonane, chalcogran (cf. Scheme 4); 3.5 m×4 mm I.D. stainless steel column filled with 120 mg **14** and 2 g squalane impregnated on 12 g Chromosorb (W-AW-DMCS, 60–80 mesh) at 70 °C and 1.8 bar dinitrogen. I: 0.2 μl injected, II: 2.0 μl injected without temperature-programming, III: *ibid.* with temperature programming [22,61].

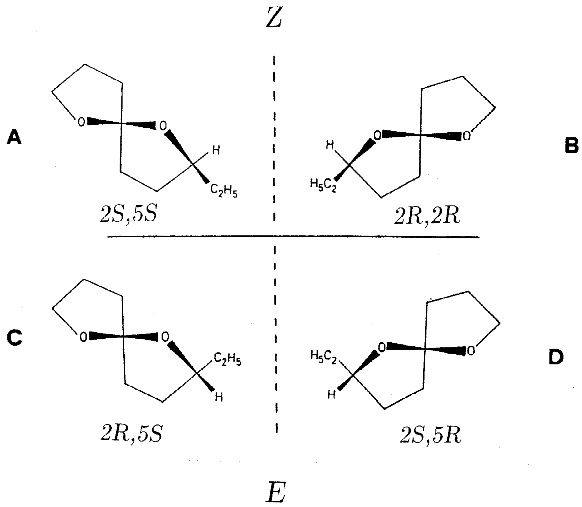

Scheme 4. Configurations of the four stereoisomers of 2-ethyl-1,6-dioxaspiro[4.4]nonane, chalcogran, the aggregation pheromone of the bark beetle *Pityogenes chalcographus* (*L.*).

rate] [65]. Although a consistent relationship between the order of elution and absolute configuration of oxiranes have been observed with 11 nickel(II) selectors (**4a, 8–17** of Scheme 5) [66], remarkable inconsistencies to the rule have also been detected [20,21]. Assignments by analogy, if made at all, should be confined to measurements at the same temperature, since peak inversions may arise at different temperatures as the result of enthalpy vs.

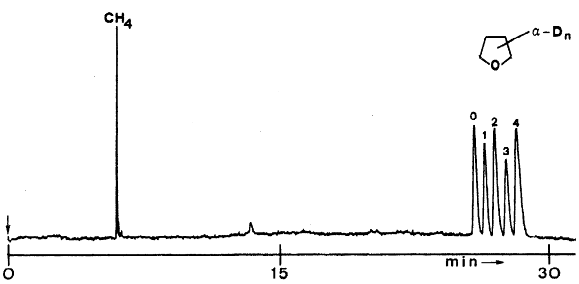

Fig. 13. Isotopic separation of α-deuterated tetrahydrofurans $C_4H^{\alpha}_{4-n}D^{\alpha}_n\,H^{\beta}_4O$ by complexation GC. 60 m×0.25 mm I.D. glass capillary column coated with 0.1 *m* cobalt(II)–*bis*[3-(heptafluorobutanoyl)-(1*R*)-camphorate] **4b** in dimethylpolysiloxane (OV 101), 0.2 μm). Oven temperature 70°C; inlet pressure 1.9 bar dinitrogen. Order of elution d_0-THF, α-d_1-THF, αα′-d_2-THF (two diastereomers), ααα′-d_3-THF,ααα′α′-d_4-THF, peak assignment by GC–MS [62].

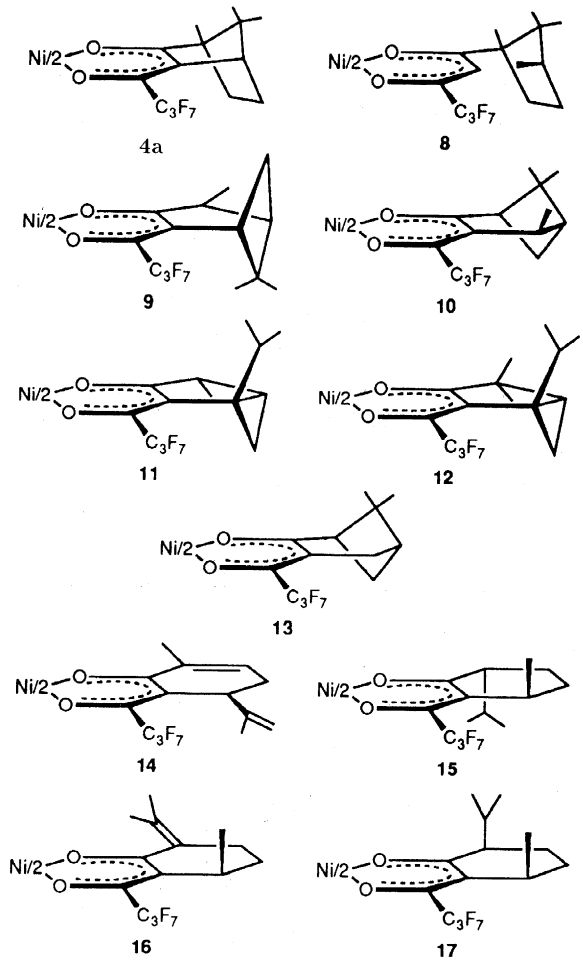

Scheme 5. Structures of 11 nickel(II) *bis*(heptafluorobutanoyl-terpeneketonates) obtained from camphor **4a**, campholylmethane **8**, pinan-3-one **9**, pinan-4-one **10**, thujan-3-one **11**, 4-methylthujan-3-one **12**, nopinone **13**, carvone **14**, menthone **15**, pulegone **16** and isomenthone **17** [66].

entropy compensation in enantiorecognition. Thus changes of the elution order of the enantiomers of, e.g. isopropyloxirane below/above the isoenantioselective temperature $T_{isoenant}$ (*peak inversion of the second kind*, cf. Section 2.6) can falsify predictions of absolute configuration by complexation GC.

1.9. Precision and sources of error of complexation GC in the analysis of enantiomers

In the course of the longstanding experience with complexation GC, some observations and recommendations pertinent to precision and sources of error in the chromatographic analysis of enantiomers have emerged [64,21]. The precision of determination of enantiomeric ratios (*er*) (or re-calculated enantiomeric excesses *ee* [67]) by complexation GC is high [19]. This statement holds not only for small enantiomeric compositions (differentiation of a true racemate from slightly enantiomerically enriched mixtures, e.g. in reactions devoted to the amplification of optical activity under prebiotic conditions) but also for very high enantiomeric ratios with 0.1–1% (and less) of enantiomeric impurities present. In Fig. 14 (left) the experimentally observed *er* of 1.000 (area 49.487/49.487) for racemic *trans*-2,3-dimethyloxirane is beyond expectation. In Fig. 14 (right) an $ee > 99$ for the enantiomerically pure oxirane can be clearly discerned [21].

It is always advantageous when the minor enantiomer is eluted as the *first* peak. This is achieved by the proper selection of the CSP which is available in both enantiomeric forms obtained from (+)- and (−)-camphor (cf. Section 1.2). Despite the success of enantioselective complexation GC for determining enantiomeric ratios *er*, potential sources of error should be mentioned [21,64]:

(i) decomposition of the sample on achiral parts of the column (the enantiomer which spends a longer time in the column will be lost preferentially causing an error in *er*)
(ii) decomposition of the sample on the chiral stationary phase (this chemical change may proceed *enantioselectively* causing the preferential loss of *one* enantiomer)
(iii) co-elution of impurities spuriously increasing peak-areas
(iv) fractionation of enantiomers by the EE-effect [68] during sample manipulation (the scalar physical properties of enantiomers may vary with the enantiomeric composition)

PEAK#	AREA%	RT
1	1.027	1.5
2	---→ 49.487	4.33
3	——→ 49.487	4.98
TOTAL	100.	

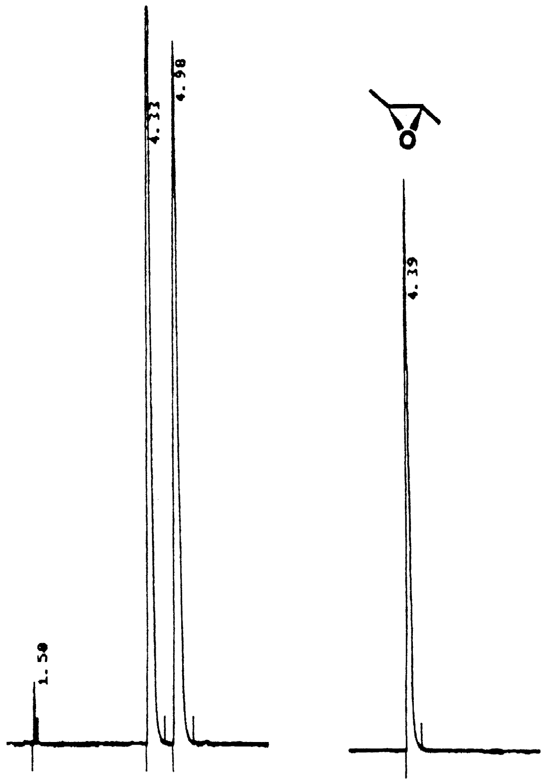

Fig. 14. Determination of the enantiomeric compositions of *trans*-2,3-dimethyloxirane separated by complexation GC on **3a**. Left: racemic *trans*-2,3-dimethyloxirane, right: (2*R*,3*R*)-*trans*-2,3-dimethyloxirane [21].

(v) enantiomerization of configurationally labile molecules producing peak distortions due to inversion of configuration during enantiomer separation (cf. Section 2.7)
(vi) peak distortions caused by an inadequate instrumentation and non-linear detector response
(vii) adsorption of both enantiomers on the column wall, leading generally to diminished peak area of the first-eluted enantiomer as a result of preferential deactivation of the adsorptive sites with the first eluted enantiomer.

A serious error in the determination of enantiomeric compositions can be caused by preferential decomposition of one enantiomer during its residence time in the column. Decomposition of the sample on achiral parts of the column will have the effect that the enantiomer which spends a longer time in the column will be lost preferentially and, as a consequence, the *er* will be biased in favour of the first eluted enantiomer. This effect can be recognized by a deviation from the expected 1:1 ratio for a racemic mixture, whereby the peak area of the second peak will be diminished. Decomposition of the sample on the chiral stationary phase will also have the effect that the enantiomer which spends a longer time in the column will be lost preferentially and *er* will be biased in favour of the first eluted enantiomer. If the decomposition is catalyzed by the chiral stationary phase in an enantioselective way, not only the second but also the first peak can be diminished.

Examples for (i) and (ii) have been detected under certain experimental conditions for reactive and/or strained chiral oxiranes separated by complexation gas chromatography (Ref. [21] and examples shown therein). In one case the second peak, and in another case the first peak was diminished for the *racemic* sample. In the latter case (cf. Section 2.8, Fig. 31), two enantioselective processes are mediated by the chiral metal complex, i.e. chromatographic resolution and kinetic resolution in favour of the first eluted enantiomer. Since two enantioselective processes are involved the elution profile will be the same when the configuration of the metal chelate is inverted. The error in *er* due to decomposition of the sample can be reduced if the difference of the residence time in the column is minimized for both enantiomers. This goal may be realized when short columns, high pressure drops, elevated temperatures and chiral stationary phases exhibiting only small separation factors α are employed. A rather trivial cause for the deviation from the expected 1:1 ratio of a racemic mixture consists of the co-elution of impurities (which may be identified by the use of a mass spectrometric detector) spuriously increasing peak areas.

Errors due to (i), (ii) and (iii) can be recognized by conducting the determination of *er* with stationary phases of opposite configuration. Errors due to (iii) can also be recognized, and eliminated, by changing the chromatographic parameters such as temperature or carrier gas flow. When the racemate is available, verification of the expected 1:1 ratio upon gas chromatographic enantiomer separation is strongly recommended in the analysis of enantiomers.

Deviations from the original *er* of a mixture of enantiomers may in principle arise during sample manipulation via self-association of the enantiomers under non-ideal conditions (‘‘EE-effect’’ [68]). This effect, *whereby the relative amounts of two enantiomers induce an observable difference between them* [68], may well lead to accidental fractionation of enantiomers during work-up, isolation or chromatographic separation. Clearly, on-column injection will avoid this source of error.

Enantiomerization of chiral samples possessing labile elements of chirality (centers, axes or planes) may undergo a change of configuration during enantiomer separation as described in Section 2.7. The resulting characteristic chromatographic peak profiles of interconversion will bias the *er*.

The detector response to a *racemic* mixture of enantiomers is strictly 1:1, since enantiomers cannot be distinguished in an achiral environment and a racemic composition (obtained by synthesis in an achiral environment) represents an ideal equimolar mixture hardly to be substituted by manually mixing any of two components. Thus the racemate can be used to test the precision of integration devices (cf. Fig. 14). In enantiomer analysis a *linear* detector response is indispensible. Thus for the correct determination of, e.g. 0.1% of an enantiomerically impurity, linearity within a concentration range of at least three orders of magnitude is required. The flame ionization detector (FID) fulfils this requirement whereas the linear response range of the electron capture detector (ECD) is low. Values obtained for *er* should therefore be verified via dilution experiments.

1.10. Accuracy of enantiomer analysis by NMR vs. complexation GC

The accuracy of the two methods of enantiomer analysis, i.e. by NMR-spectroscopy, employing chiral lanthanide(III) shift reagents, and by complexation GC, employing chiral transition metal(II) stationary phases, have been checked for methyl 2-chloropropanoate [64], an important chiral intermediate for pesticide synthesis. Thus the most efficient chiral auxiliary compounds for NMR and complexation GC, differing only in the substituent on the C1-position of camphor, were selected. According to Fig. 15 the (externally) enantiotopic carboxymethyl (singlet) and methyl groups (doublet) are well distinguished in the presence of europium(III) *tris*[(3-heptafluorobutanoyl)-10-methyl-camphorate], a derivative of **2**, by ^{1}H-NMR and the enantiomers are well separated in the presence of nickel(II) *bis*[3-(heptafluorobutanoyl-(1*R*)-10-methylene-camphorate], **5a**, by complexation GC. The auxiliaries were used in both enantiomeric forms causing peak reversals. Thus a total of four independent measurements were carried out at arbitrary enantiomeric compositions of methyl-2-chloropropanoate [64] (cf. Fig. 15). Noteworthy is the excellent agreement observed for a nearly enantiomerically pure sample (enriched by recrystallization steps) consisting of 0.2% enantiomeric impurity only, both by GC and NMR[4]. This experiment demonstrates the high degree of accuracy of these two complementary methods of the modern analysis of enantiomers.

2. Theory

2.1. Introduction

Enantioselectivity is defined as $-\Delta_{D,L}(\Delta G)$ and is frequently correlated with the chiral separation factor α[5].

$$-\Delta_{D,L}(\Delta G)\ \{=\}\ RT\ln\alpha = RT\ln(k'_D/k'_L) \qquad (1)$$

In complexation GC, the chiral selector is either diluted in, or chemically bonded to, an achiral stationary matrix (squalane, dimethylpolysiloxane). Since the solvent itself does not participate in enantiorecognition but invokes the same retention to the enantiomers it is mandatory to separate achiral and chiral contributions to retention in chromatographic selector-selectand systems displaying enantioselectivity [26,69]. Specifically it was stated *that Eq.* (1) *does not appear to have a chemical meaning in the present case, since k′ is the sum of two contributions to retention, i.e. firstly, the* (*indentical*) *physical partition of the two enantiomers between the gaseous and liquid phases and, secondly, the* (*different*) *chemical diastereomeric equilibration between the enantiomers and the optically active metal chelate in the liquid phase* [69].

Thus caution should be exercised when α is used as a criterion for enantioselectivity according to Eq. (1). Nonetheless, Eq. (1) is almost exclusively used in chiral chromatography despite a note of Pirkle et al. who reasoned for chiral bonded phases in LC that *additional retention mechanisms other than those responsible of chiral recognition attenuate the* α *value and hence stability differences between diastereomeric solvates calculated from observed* α *values will represent minimum values* [70]. A related argument of distinguishing non-selective from selective interactions in chiral LC utilizing protein stationary phases has also been advanced by Allenmark [71]. The topic has been reiterated recently by the urgent need to differentiate between apparent and true enantioselectivity in enantioseparations [72].

In enantioselective complexation GC, the concept of the *retention-increment R′* can be used to quantitatively differentiate between *physical* contributions to retention arising from achiral gas–liquid partition-

[4] In the 0.2% enantiomeric impurity range the GC experiment is much easier to perform and, therefore, in the NMR experiment only one measurement has been performed, cf. Fig. 15, bottom.

[5] The subscripts D, *dextro, right*, and L, *levo, left*, denote enantiomers, irrespective of their absolute configuration. D is arbitrarily eluted after L from the column below $T_{isoenant}$ (cf. Section 2.6). R = gas constant and T = absolute temperature, k' = retention factor.

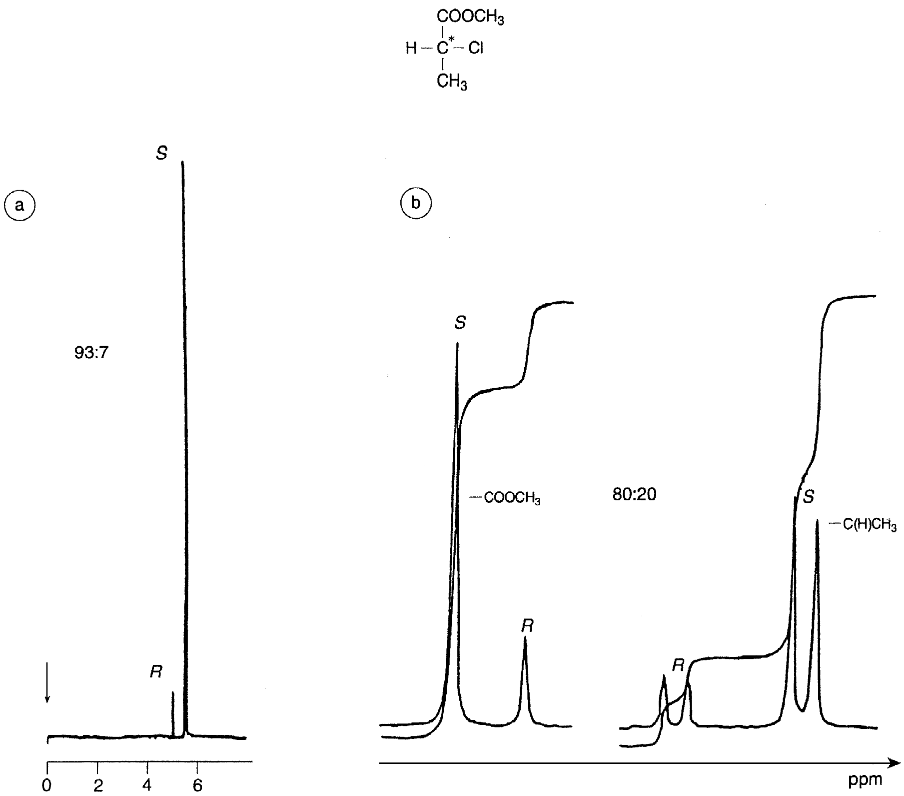

ⓐ $M=Ni/_2$; $R = CH{=}CH_2$ ⓑ $M=Eu/_3$; $R=C_2H_5$

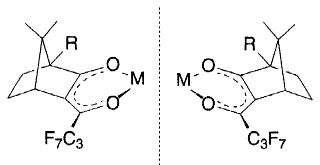

Material Analyzed	GC		NMR	
	S-Auxiliary	*R*-Auxiliary	*S*-Auxiliary	*R*-Auxiliary
rac	50.1	50.0	50.1	49.9
~80:20	80.1	80.1	80.2	80.2
~97:3	96.8	96.8	96.9	96.8
pure	99.8	99.8	–	99.8

Fig. 15. Comparison of enantiomeric compositions of methyl 2-chloropropanoate (in% of the *S*-enantiomer) by *(a) complexation GC* in the presence of nickel(II) *bis*[3-(heptafluorobutanoyl)-1-methylene-camphorate], **5a** (auxiliary used as both enantiomers), shown for the ratio of 93:7 and by *(b)* ^{1}*H-NMR spectroscopy* in the presence of europium(III) *tris*[3-(heptafluorobutanoyl)-1-methyl-camphorate], a derivative of **2** (auxiliary used as both enantiomers), shown for the ratio of 80:20) [64].

ing and *chemical* contributions to retention arising from chiral molecular complexation whereby only the latter contribution leads to the separation of enantiomers [69]:

$$-\Delta_{D,L}(\Delta G) = RT \ln(R'_D/R'_L) \tag{2}$$

It is even possible to extrapolate the achiral contribution to retention when a given pair of enantiomers is separated on two columns with different concentrations of the chiral selector.

2.2. The concept of the retention-increment R′

Consider a volatile selectand B migrating through a complexation column containing a dilute solution of the non-volatile selector A as an additive in the non-volatile solvent S (cf. Fig. 16, right).

When a 1:1 complex is formed[6] rapidly and reversibly between A and B, two equilibria can be distinguished

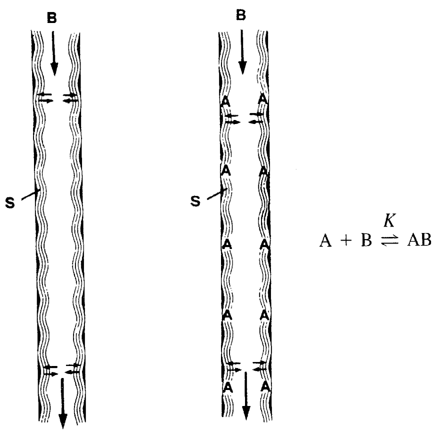

$$k'^{\circ} = \frac{t'^{\circ}_R}{t^{\circ}_M} - 1 = K^{\circ}_L \frac{1}{\beta^{\circ}} \quad (9) \qquad R' = \frac{K_L}{K^{\circ}_L} - 1 = K\, a_A \quad (8)$$

Fig. 16. The principle of complexation GC. Left: Reference column containing the pure solvent S. Right: Complexation column containing the selector A in the solvent S. Retention parameters refer to the selectand B.

[6]Since the selectand B is employed in high dilution vis-a-vis the selector A, the occurrence of an exclusive 1:1 complexation equilibrium is plausible.

$$B_{(g)} \rightleftharpoons B_{(l)} \quad \text{or} \quad K_L{}^{\circ} = \frac{c_{B(l)}}{c_{B(g)}} \tag{3}$$

and

$$A + B_{(l)} \rightleftharpoons AB \quad \text{or} \quad K = \frac{a_{AB}}{a_A a_{B(l)}} = \frac{c_{AB}}{c_A c_{B(l)}} \frac{\gamma_{AB}}{\gamma_A \gamma_{B(l)}} \tag{4}$$

where the subscripts g and l refer to the gas and the liquid phase, respectively. $K_L{}^{\circ}$ is the distribution constant (partition coefficient) of B between the gas and the pure liquid phase S neglecting the presence of A diluted in S (note that $K_L{}^{\circ}$ quantifies the *physical contribution to retention*). K is the thermodynamic complexation constant of A and B in S (note that K quantifies the *chemical contribution to retention*) and a_i is the activity of the species i, with the convention that $a_i \rightarrow c_i$ at high dilution in the solvent S, i.e. $c \rightarrow 0$. As the amount of $B_{(l)}$ injected (and therefore AB formed) is very low in the gas-chromatographic experiment, Eq. (4) can be rewritten

$$K\, a_A = \frac{c_{AB}}{c_{B(l)}} \tag{5}$$

The total concentration of selectand B present in the liquid phase S is $c_{B(l)} + c_{AB}$. Hence, the *apparent* distribution constant K_L, assuming no volume change on dissolution of B, is [5]

$$K_L = \frac{c_{B(l)} + c_{AB}}{c_{B(g)}} \tag{6}$$

With Eqs. (3) and (5) the expression (6) can be rewritten

$$K_L = \frac{c_{B(l)}}{c_{B(g)}} + \frac{c_{AB}}{c_{B(g)}} = \frac{c_{B(l)}}{c_{B(g)}} + \frac{c_{B(l)}}{c_{B(g)}} \frac{c_{AB}}{c_{B(l)}} = K_L{}^{\circ} + K_L{}^{\circ} K\, a_A \tag{7}$$

or

$$K\, a_A = \frac{K_L}{K_L{}^{\circ}} - 1 \tag{8}$$

Thus the thermodynamic complexation constant K can be obtained from the plot of K_L vs. a_A (Eq. (7)) [5–7].

From Eq. (8) a very useful relationship between K and chromatographic retention data can be developed when a reference column is employed containing the pure solvent S (cf. Fig. 16, left)[7] and an inert non-complexing reference compound B* (e.g. a saturated hydrocarbon) is co-injected with B [9,10,31][8].

The distribution constant of the selectand B between the gas and the pure liquid phase S in the reference column, $K_L{}^\circ$, is defined by

$$K_L{}^\circ = k'^\circ \beta^\circ \tag{9}$$

and the *apparent* distribution constant of the selectand B between the gas and the liquid phase S containing the selector A in the complexation column, K_L, is defined by

$$K_L = k' \beta \tag{10}$$

where k'° is the retention factor of B in the pure solvent S in the reference column, k' is the retention factor of B in the solution of A in S in the complexation column, β° is the phase ratio of the reference column and β is the phase ratio of the complexation column. Eq. (8) can now be rewritten

$$K\,a_A = \frac{k'}{k'^\circ}\,\frac{\beta}{\beta^\circ} - 1 \tag{11}$$

For the non-complexing reference compound B* (e.g. an inert saturated hydrocarbon) it is required that $K^* = 0$. From Eq. (11), it follows for B* that

$$\frac{k'^*}{k'^{\circ *}}\,\frac{\beta}{\beta^\circ} = 1 \tag{12}$$

The ratio β/β° is equal for B and for co-injected B* and Eqs. (11) and (12) are combined to

$$K\,a_A = \frac{k'}{k'^\circ}\,\frac{k'^{\circ *}}{k'^*} - 1 \tag{13}$$

With

$$\frac{k'^\circ}{k'^{\circ *}} = \frac{t_R'{}^\circ}{t_R'{}^{\circ *}} = r^\circ \tag{14}$$

and

$$\frac{k'}{k'^*} = \frac{t_R'}{t_R'{}^*} = r \tag{15}$$

[7]Symbols referring to the reference column are marked with a circle, e.g. $K_L{}^\circ$, k'°.

[8]Symbols referring to B* are marked with an asterisk, e.g. k'^*.

a relationship reminiscent of Eq. (8) but referring now to *relative* retention data r° and r is obtained

$$K\,a_A = \frac{r}{r^\circ} - 1 = \frac{r - r^\circ}{r^\circ} = R' \tag{16}$$

where r is the relative retention of the selectand B with respect to the inert reference compound B* in a complexation column containing the selector A with the activity a_A in the inert solvent S (cf. Fig. 16, right), and r° is the relative retention of the selectand B with respect to the same reference compound in the reference column containing the pure solvent S, devoid of the selector A (cf. Fig. 16, left).

The quantity R' is called the *retention-increment* (previously named retention-increase [31]) of B. R' is a quantitative measure of complexation between A and B in S. Thus $1/(1 + R')$ represents the fraction of the selectand B dissolved in the solvent S whereas $R'/(1 + R')$ defines the fraction of the selectand B complexed with the selector A. Hence R' is proportional to the thermodynamic complexation constant K.

Whereas it is experimentally difficult to determine the phase ratios β and β° according to Eq. (11) of two separate columns, the relative retention data r° and r in Eq. (16) are independent of all operating conditions (column dimensions, flow-rate and film thickness) except the temperature. Only the gas-phase hold-up time t_M of the two columns has to be known precisely to calculate adjusted retention times t_R' according to Eqs. (14) and (15) (either taken as the time of the air peak, if present, or, as an approximation, determined from the peak of co-injected methane).

According to Eq. (16), the retention-increment R' is linearly related to a_A at a given temperature when a 1:1 molecular complex is formed between A and B. A similar approach has been advanced in argentation GC [73,74]. As the high concentration of silver nitrate in ethylene glycol was critical due to a salting-out effect [6], lithium nitrate dissolved in ethylene glycol has been used as the reference column. Again, the use of an inert reference compound greatly facilitated the approach.

The formal similarity between the basic equation of chromatography, Eq. (9), describing the chromatographic process in the reference column (cf. Fig. 16, left), and the derived equation of complexation chromatography, Eqs. (11) and (16), describing the chromatographic process in the complexation column (cf. Fig. 16, right), should be noted. Consequently, the retention-increment R' may also be called the *chemical retention factor* and $r°$ may be related to a *physical hold-up time* (cf. Fig. 17, *vide infra*).

The validity of Eq. (16) has been scrutinized by careful and extensive experiments [31]. Whereas the retention-increment R' can accurately be measured, an error in the *absolute* value of the thermodynamic complexation constant K according to Eq. (16) may arise due to the incertitude of the activity a_A of the selector A in the solvent S. The unknown activity a_A can be substituted by the molarity M_A or, preferably, by the molality m_A, in very diluted solutions. The unit molality is independent of the temperature, and, for practical reasons, it is advantageous to add A to the weighed amount of S [31]. Fortunately, the unknown activity a_A of the selector A in the solvent S cancels when the *ratio* of stability constants of two selectands B_X and B_Y (isomers, isotopomers, enantiomers), competing for the selector A, are compared.

The term selectivity S' is defined here as the ratio of thermodynamic complexation constants K_X/K_Y. According to Eq. (17) the selectivity S' can directly

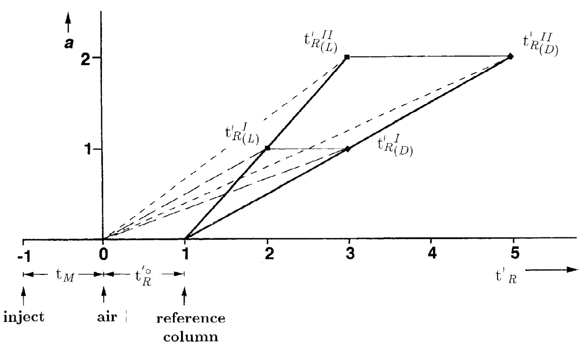

Fig. 17. Schematic representation of the distinction between (i) non-enantioselective contributions to adjusted retention times of B, t'°_R, and (ii) enantioselective contributions to adjusted retention times of B_i, $t'_{Ri} - t'^{\circ}_R$ (i=L and D denoting enantiomers of B), leading to the constancy of the ratio of R'_D/R'_L as required by Eq. (18) (for simplification relative retentions r are replaced by adjusted retention times t'_R. t_M, t'_R and t'°_R were arbitrarily set unity, the ratio R'_D/R'_L was set 2. t'_{Ri} represents arbitrary numbers. Real measured figures for *E*-chalcogran are quoted in the text. The arbitrary concentrations c (or activities a) of A were set 1 and 2, respectively) [79].

be related by the ratio of the retention-increments R' of the selectands B_X and B_Y competing for the selector A. The selectivity S' and it is thus independent of the activity of A in S, a_A.

$$S'_{X,Y} = \frac{K_X}{K_Y} = \frac{R'_X}{R'_Y} = \frac{r_X - r_X{}^{\circ}}{r_Y - r_Y{}^{\circ}} \cdot \frac{r_Y{}^{\circ}}{r_X{}^{\circ}} \tag{17}$$

Thus as derived above, only relative retention data $r_X{}^{\circ}$, $r_Y{}^{\circ}$, r_X and r_Y have to be measured for the determination of thermodynamic data of competing selectands B_X and B_Y using a reference column containing the pure solvent S, devoid of the selector A, and a complexation column containing A in S (cf. Fig. 16).

2.3. The determination of the enantioselectivity $-\Delta_{D,L}(\Delta G)$ from the retention-increment R'

An interesting situation arises in complexation GC when enantiomers B_D and B_L are considered. B_D and B_L are distinguished in a chiral environment and may be separated when the selector A is chiral and non-racemic. Significantly, as enantiomers can not be discriminated on the achiral reference column, $r°$ is identical for B_D and B_L. Hence, Eq. (17) can be simplified to

$$S'_{D,L} = \frac{K_D}{K_L} = \frac{R'_D}{R'_L} = \frac{r_D - r^{\circ}}{r_L - r^{\circ}} \tag{18}$$

Since the enantiomers B_D and B_L compete for the same selector A in S, the ratio K_D/K_L is directly related to the ratio of their retention-increments R'_D/R'_L accessible from relative retention-data r_D, r_L and $r°$. As outlined above, this ratio is independent of the activity of A in S, a_A, and thus of the concentration of the selector. Since $r°$ is identical for the enantiomers B_D and B_L, its value can even be extrapolated from two sets of data for the relative retention, r, of the enantiomers B_D and B_L at two arbitrary concentrations (1 and 2) of A in S as a consequence of the Eq. (16).

$$r_0 = \frac{r_D^{(1)} r_L^{(2)} - r_L^{(1)} r_D^{(2)}}{\left(r_D^{(1)} + r_L^{(2)}\right) - \left(r_L^{(1)} + r_D^{(2)}\right)} \tag{19}$$

Significantly, Eq. (19) can be used to calculate non-enantioselective contributions to retention when t'°_R (or $r°$, respectively) is not readily accessible due to the inavailability of the solvent S to prepare a reference column, e.g. with polysiloxane-anchored chiral selectors such as Chirasil-Metal **6** and **7** (cf. Section 1.4) or with various chiral stationary phases used in LC in which the enantioselective center of the selector is diluted by non-enantioselective interaction sites including those of the support.

The validity of Eq. (19) has been verified with great care [53]. Thus the enantiomers of *E*-2-ethyl-1,6-dioxaspiro[4.4]nonane, *E*-chalcogran (configuration, cf. Scheme 4), exhibited the following relative retentions (in respect to *n*-dodecane at 93 °C) on a 25 m×0.25 mm I.D. fused-silica column coated with two (arbitrary) concentrations (1) and (2) of nickel(II) *bis*[3-(heptafluorobutanoyl)-(1*R*)-camphorate] in SE 54 polysiloxane: $r_L^{(1)}=0.95$ and $r_D^{(1)}=1.13$ as well as $r_L^{(2)}=1.90$ and $r_D^{(2)}=2.44$. $r°$ is calculated to 0.475 according to Eq. (19). Measurements of $r°$ at a reference column coated with pure SE 54 between 80 and 120 °C at intervals of 5 °C yielded an extrapolated value for $r°$ of 0.476±0.001 at 93 °C which is in excellent agreement with the calculated figure. The essence of Eq. (19) is graphically depicted in Fig. 17 which highlights also the role of $t_R'°$ (or $r°$, respectively) as *physical* hold-up time. In fact, the complexation chromatogram has its origin in the adjusted retention time $t_R'°$ (or $r°$, respectively). Starting from this point, the *chemical* retention of the enantiomers L and D of the selectand B increase linearly with the increase of the activity (concentration) a_A of the selector A.

Enantioselectivity is defined as the Gibbs energy (free enthalpy) difference $-\Delta_{D,L}(\Delta G)$ of the transient diastereomeric complexes AB_D and AB_L. By combining Eq. (18) and the Gibbs–Helmholtz-equation, the modified Eq. (2) is derived in its correct form, Eq. (20), which separates non-enantioselective and enantioselective contributions to retention

$$-\Delta_{D,L}(\Delta G) = -\Delta_{D,L}(\Delta H) + T\Delta_{D,L}(\Delta S) = RT\ln S'_{D.L} = RT\ln\frac{K_D}{K_L} = RT\ln\frac{R'_D}{R'_L} = RT\ln\left(\frac{r_D - r°}{r_L - r°}\right) \quad (20)$$

Thus the thermodynamic parameters $-\Delta_{D,L}(\Delta G)$, $-\Delta_{D,L}(\Delta H)$ and $\Delta_{D,L}(\Delta S)$ of enantioselectivity can be obtained by van't Hoff plots when measurements are performed at different temperatures T according to

$$R\ln\frac{R'_D}{R'_L} = \frac{-\Delta_{D,L}(\Delta G)}{T} = -\frac{\Delta_{D,L}(\Delta H)}{T} + \Delta_{D,L}(\Delta S) \quad (21)$$

As a thermodynamic quantity, $-\Delta_{D,L}(\Delta G)$ is strictly independent of the activity a_A of A in S and, hence, also of its concentration (molality). It has previously been verified in complexation GC that isothermal measurements at different concentrations of the selector A yielded the same value for $-\Delta_{D,L}(\Delta G)$ at a very high level of confidence [53,66] (an example is provided in Section 2.6.). Even concentration gradients of A in S[9] do not affect $-\Delta_{D,L}(\Delta G)$.

The ratio R'_D/R'_L of a chiral selectand B depends on the enantiomeric purity of the selector A. The maximum $-\Delta_{D,L}(\Delta G)$ refers to an enantiomerically pure chiral selector A (*ee*=100%). When A is not enantiomerically pure (*ee*<100%) the relative retention r_{ee} (measured with A of given *ee*) can be extrapolated to r_{100} (corresponding to *ee*=100%) via Eqs. (22) and (23) [66,75]:

$$r_{D_{100}} = \frac{1}{2}(r_{D_{ee}} + r_{L_{ee}}) + \frac{50}{ee}(r_{D_{ee}} - r_{L_{ee}}) \quad (22)$$

and

$$r_{L_{100}} = \frac{1}{2}(r_{D_{ee}} + r_{L_{ee}}) - \frac{50}{ee}(r_{D_{ee}} - r_{L_{ee}}) \quad (23)$$

with

$$ee(\%) = \frac{D-L}{D+L}\cdot 100 \quad (24)$$

Note that the second part in Eqs. (22) and (23) requires for $ee \to 0$ (racemic selector), $r_D - r_L \to 0$ (no separation of the enantiomers, *peak coalescence of the second kind*, cf. Section 2.11). This derivation is based on the reasonable assumption that *ee* of A is linearly related to $-\Delta_{D,L}(\Delta G)$. Non-linear relation-

[9]Concentration gradients may be formed when columns containing the polysiloxane solvent S being chemically bonded to the surface, e.g. CB-fused-silica columns, are impregnated (doped) with A by dynamic coating.

ships as observed in enantioselective catalysis [76,77] are in principle also possible in enantioselective chromatography but have never been described[10].

2.4. The erroneous use of the separation factor α as measure of enantioselectivity $-\Delta_{D,L}(\Delta G)$ in the presence of non-enantioselective contributions to retention

Selectivity S' in GC is customarily described by the separation factor α. For practical reasons, this applies also for enantiomers according to

$$\alpha = \frac{k'_D}{k'_L} = \frac{t'_D}{t'_L} = \frac{r_D}{r_L} \tag{25}$$

In enantioselective complexation GC and related techniques, the separation factor α_{dil} is rendered concentration-dependent when A is diluted in S [78]. By substituting r_D and r_L in Eq. (25) by Eq. (16) with r° being equal for enantiomers it follows that [78]

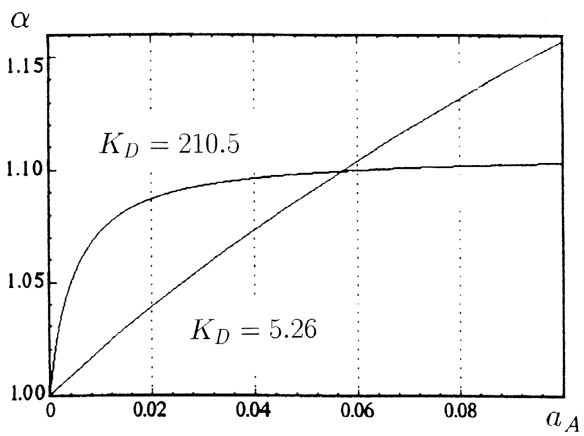

Fig. 18. Simulated plot of α vs. a_A. Curve 1: $K_D = 5.26$; curve 2: $K_D = 210.5$ (for $a_A = 0.057$ the same $\alpha = 1.10$ results when $R'_D = 0.3$ and $R'_D = 12$, respectively) [78].

[10] This phenomenon is expected to arise when the selector A is prone to dimerization as for **3a** and **4a**. In the hypothetical case that only heterochiral dimers are formed quantitatively being inactive toward complexation, the remaining major enantiomer of the monomer would solely be responsible in determining $-\Delta_{D,L}(\Delta G)$ even at enantiomeric mixtures of low *ee*.

$$\alpha_{dil} = \frac{K_D a_A + 1}{K_L a_A + 1} = \frac{R'_D + 1}{R'_L + 1} \tag{26}$$

According to Eq. (26), α depends on the activity (concentration) a_A. The optimum of α is reached already at low concentrations if chemical complexation is strong (i.e. large K or $R' \gg 1$). A simulated plot of α vs. a_A for the arbitrary values $K_D = 5.26$ and $K_D = 210.5$ according to Eq. (26) is shown in Fig. 18 [78].

Thus the separation factor α is an inappropriate quantity to describe enantioselectivity $-\Delta_{D,L}(\Delta G)$ in diluted systems according to Eq. (1). Its numerical value *underestimates* the chiral discrimination ability of A since the retention factor k' from which it is calculated is the sum of the non-enantioselective (physical) contribution to retention, r°, and the enantioselective (chemical) contribution to retention $r_i - r^\circ$. It is only the ratio of the latter which leads to the separation of enantiomers according to Eq. (20), i.e. $(r_D - r^\circ)/(r_L - r^\circ)$. This notion is confirmed by the experiment. The enantioselectivity of *E*-2-ethyl-1,6-dioxaspiro[4.4]nonane, chalcogran (cf. Scheme 4) at 93 °C calculated by Eq. (20) using the relative retentions quoted in Section 2.3 [53] is $-\Delta_{D,L}(\Delta G) = 0.234$ kcal/mol at the low selector concentration (1) and $-\Delta_{D,L}(\Delta G) = 0.234$ kcal/mol at the high selector concentration (2), respectively. Using the inappropriate Eq. (1), $-\Delta_{D,L}(\Delta G)$ is underestimated and is rendered concentration-dependent, i.e. $-\Delta_{D,L}(\Delta G) = 0.126$ kcal/mol at the low selector concentration (1) but $-\Delta_{D,L}(\Delta G) = 0.182$ kcal/mol at the high selector concentration (2), respectively. $-\Delta_{D,L}(\Delta G)$ can be approximated from Eq. (27) valid for undiluted selectors A (cf. Eq. (1) [75] only in the rare case when r° is very low and complexation is very strong, i.e. $r \gg r^\circ$,

$$-\Delta_{D,L}(\Delta G) = RT \ln \alpha_{undil} \sim RT \ln \frac{t'_{R_D}}{t'_{R_L}} \sim RT \ln \frac{r_D}{r_L} \quad \text{for } r \gg r^\circ \tag{27}$$

The validity of Eq. (20) has also been corroborated by the gas-chromatographic separation of enantiomers using diluted cyclodextrin selectors [79–81].

2.5. Mechanistic aspects of the separation of enantiomers by complexation GC – the elusive concept of an enantiorecognition factor χ

From a chromatogram displaying the separation of enantiomers by complexation GC useful information can be obtained from the peak parameters displayed in Scheme 6 [20,36].

Thermodynamic data describing chemical selectivity and enantioselectivity (cf. (1) and (2) in Scheme 6) are obtained from relative retention data r and $r°$ by complexation gas chromatography according to Eqs. (16) and (20) [20,28,36]. In a comprehensive effort, the complexation equilibria between 15 chiral mono-, di-, and trialkylsubstituted cyclic ethers (mainly oxiranes) and 11 chiral and non-racemic nickel(II)–*bis*-[α-(heptafluorobutanoyl)-terpeneketonates] **4a, 8–17** with different molecular architectures (cf. Scheme 5) have been measured in squalane at 60 °C in an effort to gain mechanistic insights into enantioselective complexation GC [66]. Some noteworthy trends have been observed. The selectors **4a** and **8** showed similar enantioselectivities $-\Delta_{D,L}(\Delta G)$ implying that structural rigidity was not a prerequisite for efficient enantiorecognition. The highest enantiomeric bias was obtained with the selector **12**. Not only selectors containing bicyclic molecular structures but also those with monocyclic structures, e.g. differing in the geometric relation of the 1,4-dialkyl substituents **15–17**, were efficient for the discrimination of enantiomers [66] although no obvious relationships between structure and enantioselectivity was found. Although **14** represents a planar structure with the exception of the chiral center carrying the isopropenyl group, this selector was highly enantioselective and could even be used for the efficient semipreparative separation of the enantiomers of spiroketals such as chalcogran (cf. Section 1.6.) [22,61]. Some selectors were not readily available in an enantiomerically pure form. Therefore, the maximum $-\Delta_{D,L}(\Delta G)$ was extrapolated according to Eqs. (22) and (23).

1. *Peak retention*	chemoselectivity	$-\Delta G$
2. *Peak separation*	enantioselectivity	$-\Delta_{D,L}(\Delta G)$
3. *Peak coalescence* (fourth kind)	enantiomerization barrier	$\Delta G‡$
4. *Peak ratio*	enantiomeric ratio	*er*
5. *Peak assignment*	enantiomeric configuration	*R*,*S*

Scheme 6. Four peak parameters in enantioselective complexation GC [20].

When enantioselective complexation GC was devised it was though that the prerequisite to efficient enantioselectivity $-\Delta_{D,L}(\Delta G)$ was a strong complexation strength $\Delta G_{mean} = 1/2(\Delta G_L + \Delta G_D)$ between the selectand and the selector. In fact, this misconception delayed the advent of enantioselective complexation GC. For example, the first target of extensive investigations was concerned with the chiral olefin 3-methyl-1-pentene that exhibited a much stronger π-complexation ability with **1** as compared to 3-methylcyclopentene [9,11]. But only the cyclic olefin can be separated into enantiomers (cf. Section 1.2). Also for chiral aliphatic oxiranes, no relationship between the strength of molecular complexation of the two enantiomers, $-\Delta G_{mean}$, and the magnitude of enantiorecognition, $\Delta_{D,L}(\Delta G)$, defined as the *chiral recognition factor* χ (or enantiorecognition factor) was found with the 11 nickel(II) selectors **4a, 8–17** (cf. Scheme 6) [66]

$$\chi = -\Delta_{D,L}(\Delta G)/-\Delta G_{mean} \tag{28}$$

This trend can be demonstrated in Fig. 19 for chiral 2-methyl-substituted cyclic ethers separated on manganese(II)–*bis*[3 - (heptafluorobutanoyl) - (1*R*)-camphorate] **4c** [69].

A very high complexation selectivity, K_{rel}, differing by a factor of 65, was observed as the result of changing the ring size of the cyclic ethers, i.e.

$$\text{oxetane} \gg \text{oxolane} \geq \text{oxirane} > \text{oxane}$$

The extraordinarily strong complexation of the oxetane and metal(II) selectors, not yet understood, gives rise to extreme retention times notably for the strong acceptor nickel(II) [66]. As has been outlined in Section 2.4., the separation factor α does not represent a reliable criterion for enantioselectivity according to Eq. (1) because it ignores the different volatilities as expressed by the different values of $r°$ for the cyclic ethers. Thus it is not readily obvious from the chromatogram depicted in Fig. 19 that the

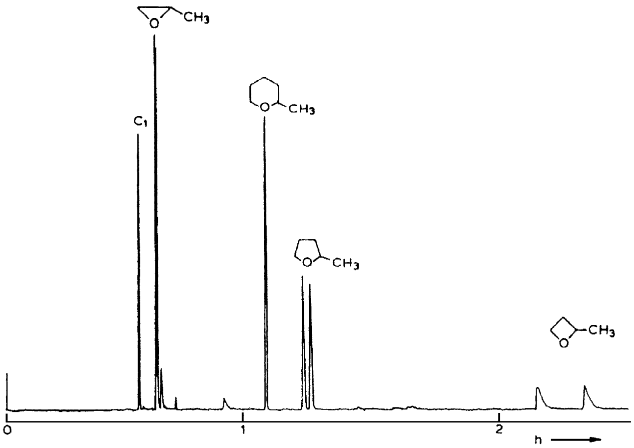

α	1.07	1.00	1.05	1.09	
K_{rel}	1	0.2	2.5	13	
$-\Delta_{D,L}(\Delta G)$	130	0	40	80	cal/mol

Fig. 19. Influence of ring size of 2-methyl-substituted cyclic ethers on α, K_{rel} (first eluted enantiomer) and $-\Delta_{D,L}(\Delta G)$ at 60 °C (160 m×0.4 mm I.D. stainless steel column coated with 0.05 *m* **3a** in squalane; carrier gas: dinitrogen) [69].

true enantioselectivity, correctly expressed by $-\Delta_{D,L}(\Delta G)$, decreases in the order

oxirane > oxetane > oxolane > oxane

Thus neither a strong complexation (for the oxetane) nor a very weak complexation (for the oxane) is essential for an efficient enantioselectivity. The highest degree of enantiorecognition is in fact observed when the complexation strength $-\Delta G_{mean}$ is intermediate, i.e. for oxiranes. Therefore, the intuitive assumption that strong molecular complexation is a prerequisite for a high enantioselectivity is not verified by the experiment. This finding appears to be of general validity in enantioselective chromatography. It applies also when the different complexation properties of the metal(II) selectors are considered. The complexation strength of the metal(II) ions for oxygen-, nitrogen- and sulfur-containing selectands increases markedly in the order [31,69]

manganese(II) < cobalt(II) ≪ nickel(II)

Yet although manganese(II) (and notably zinc(II)) are very weak acceptors compared to nickel(II), high enantioselectivities are often observed with these selectors despite the low retention-increments R' of the selectands [69]. Thus the chiral recognition factor χ, cf. Eq. (28), decreases in the order

manganese(II) > cobalt(II) > nickel(II)

For chiral alkylsubstituted oxiranes, a consistent relationship between the absolute configuration of the enantiomers and the order of elution (cf. (5) in Scheme 5) was observed for all oxiranes on **4a, 8–17** [66] in accordance with a proposed *quadrant rule* [65]. However the magnitude and the sign of enantioselectivity $\pm\Delta_{D,L}(\Delta G)$ between alkylsubstituted oxiranes and **4a, 8–17** could neither be predicted nor rationalized by simple molecular models [66]. This situation is further complicated by the temperature dependence of the enantioselective complexation equilibria (cf. Section 2.6). Thus it had been noted [69] that the enantiomers of isopropyloxirane are not separated on the nickel(II) selector **4a** but are well separated on the manganese(II) selector **4c** at 60 °C. Indeed a temperature-dependent reversal of the enantioselectivity for isopropyloxirane is described in Section 2.6. A real conundrum is the observation of a reversal of the elution order between the enantiomers

Fig. 20. Coordination geometry of aquo–pyridino–nickel(II) *bis*[3-(heptafluorobutanoyl)-(1*R*)-camphorate] **4a** [56].

of (2*S*,3*S*)-trans-2,3-dimethyloxirane and (2*S*,3*S*)-trans-2,3-dimethylthiirane on **4a** [20].

No attempts have been made thus far to model enantioselectivity in complexation GC since the structure of the dissolved selectors in the gas-chromatographic experiment (coordination geometry, oligomerization status) is not known with certainty. The nickel(II) selectors **3a** and **4a** are dimeric with two nickel atoms sharing two oxygens in a bridged structure [82]. An unusual coordination geometry was found for a complex of **4a** with water and pyridine (cf. Fig. 20) [56]. The complex was formed when a coating solution of **4a** in dimethylpolysiloxane was accidentally set aside for about a year. Pyridine must have been taken up from the air of the laboratory. A tentative coordination geometry with an oxirane will be discussed in Section 2.9. (cf. Scheme 8).

2.6. The temperature-dependence of enantioselectivity, enthalpy/entropy compensation and the isoenantioselective temperature

According to Eq. (20), the separation of enantiomers by complexation GC is entirely governed by thermodynamics at the fast kinetics of complexation. The enantioselectivity $-\Delta_{D,L}(\Delta G)$ is thus determined

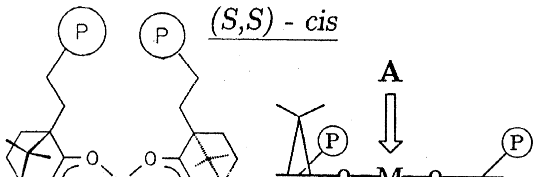

Scheme 8. Different coordination geometries of a selector (e.g. Chirasil-Nickel **7a**) and their impact to the approach of the enantiomers of a selectand (A and B symbolize coordination sites) [100].

by an enthalpy term, $-\Delta_{D,L}(\Delta H)$, and an entropy term, $\Delta_{D,L}(\Delta S)$. For a 1:1 complexation process, both terms oppose each other in determining $-\Delta_{D,L}(\Delta G)$. The resulting enthalpy/entropy compensation is due to the fact that the more tightly bonded complex ($-\Delta H_D > -\Delta H_L$) is also more ordered, i.e. $\Delta S_D < \Delta S_L$ (and vice versa for the other enantiomer). Since the entropy term increases with temperature T according to Eq. (20), the enantioselectivity $-\Delta_{D,L}(\Delta G)$ is rendered temperature-dependent. As predicted by Schurig and Koppenhoefer [26,83], $\Delta_{D,L}(\Delta G)$ becomes nil at a certain coalescence temperature called the *isoenantioselective temperature* $T_{isoenant}$ ($K_D = K_L$, no enantioselectivity)

$$T_{isoenant} = \Delta_{D,L}(\Delta H)/\Delta_{D,L}(\Delta S) \qquad (29)$$

At $T_{isoenant}$, *peak coalescence of the third kind* (cf.

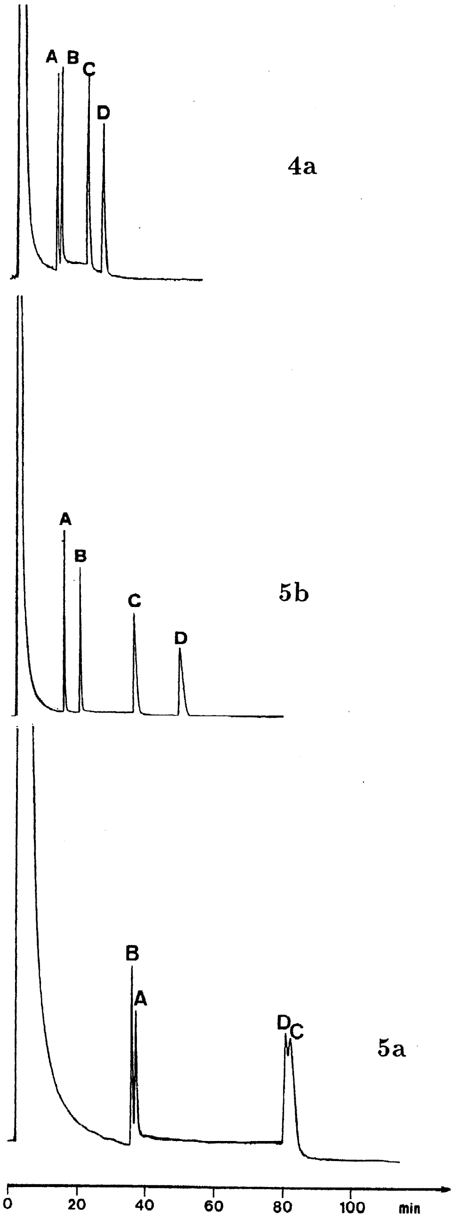

Fig. 23. Influence of structural changes at the C(10)-position of camphor in the gas-chromatographic separation of the enantiomers of *Z*- and *E*-chalcogran (A–D) (cf. Scheme 4) on **4a**, **5b** and **5a**. Top: 37 m×0.25 I.D. glass capillary column coated with 0.12 *m* **4a** in SE-54 (0.2 μm film thickness) at 80 °C, 1 bar dinitrogen. Center: 25 m×0.25 mm I.D. glass capillary column coated with 0.13 *m* **5b** in SE-54 (0.2 μm film thickness) at 80 °C, 1 bar dinitrogen. Bottom: 24 m×0.25 mm I.D. glass capillary column coated with 0.125 *m* **5a** in SE-54 (0.2 μm film thickness) at 80 °C, 1 bar dinitrogen. Peak assignment: A=(2*S*,5*S*), B=(2*R*,5*R*), C=(2*R*,5*S*) and D=(2*S*,5*R*) [53].

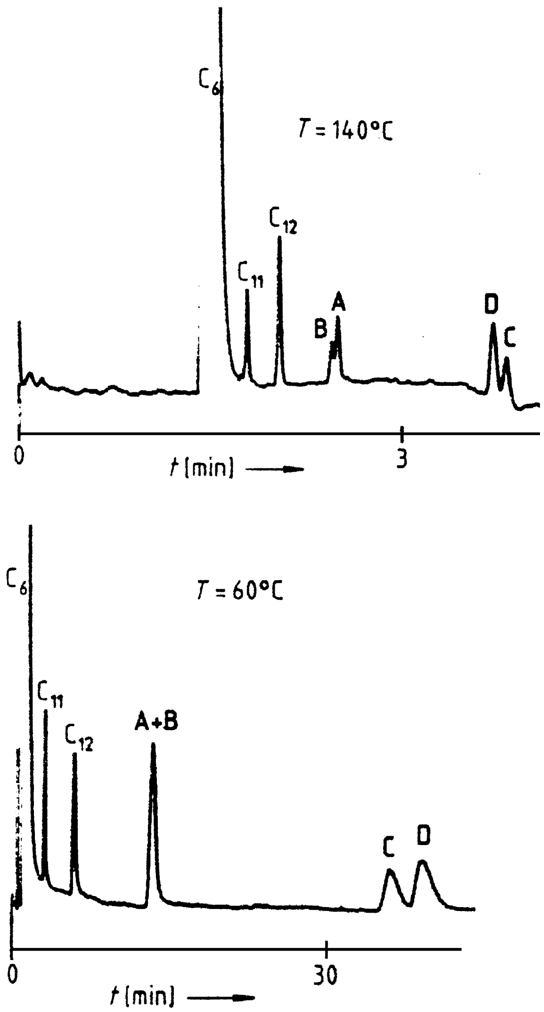

Fig. 24. Temperature-dependent reversal of the elution order of the enantiomers of *E*-chalcogran C,D (cf. Scheme 4) by complexation GC on nickel(II) *bis*[3-(heptafluorobutanoyl)-(1*S*)-10-methylene-camphorate] **5a** (for the sake of this evidence the racemic C,D mixture was enriched with the D-enantiomer [45]). 25 m×0.25 mm I.D. fused-silica column coated with 0.15 *m* **5a** in OV-101 (0.2 μm film thickness) at 140 °C (top) and 60 °C (bottom), 1 bar dinitrogen. C_6 = *n*-hexane (solvent), C_{11} = *n*-undecane and C_{12} = *n*-dodecane [84].

E-chalcogran on **5d**:
$-\Delta_{D,L}(\Delta H)=0.857$ kcal/mol
$\Delta_{D,L}(\Delta S)=-\ 2.41$ cal/K mol
$T_{isoenant}=356$ K (~82°C)

Despite different values of $-\Delta_{D,L}(\Delta H)$ and $\Delta_{D,L}(\Delta S)$ between **5d** and **5a** the plot $-\Delta_{D,L}(\Delta H)$ vs.

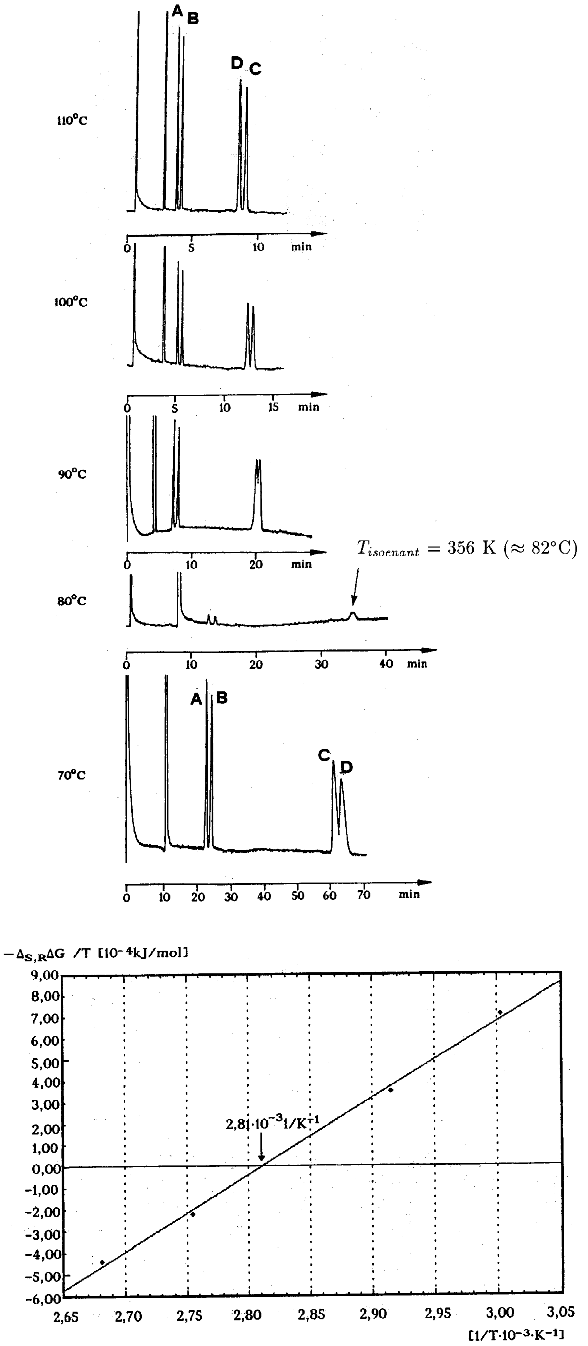

Fig. 25. Top: Temperature-dependent reversal of the elution order of the enantiomers of *E*-chalcogran C,D (cf. Scheme 4) by complexation GC on nickel(II) *bis*[3-(heptafluorobutanoyl)-1*S*)-10-isobutylidene-camphorate] **5d**. 20.5 m×0.25 mm I.D. glass capillary column coated with 0.129 *m* **5d** in OV-101 between 70 and 110 °C at 1 bar dinitrogen. Bottom: Linear van't Hoff-plot and determination of the isoenantioselective temperature $T_{isoenant}$ [27].

$\Delta_{D,L}(\Delta S)$ is constant with the slope $T_{isoenant} \sim 355$ K suggesting the same mechanism of enantiorecogniton. In line with the different thermodynamic data the predicted temperature-dependent inversion of the elution order of the enantiomers of *E*-chalcogran (C,D vs. D,C) was established on **5a** in the rather broad temperature interval of 60–140 °C [84] whereas the interval between 70 and 110 °C was already sufficient on **5d** as depicted in Fig. 25 (top). Although the selectand–selector complexation is steadily reduced between 70 and 110 °C (decrease of R'), C is first eluted *before* D at 70 °C (the separation is preferentially enthalpy-controlled), then peak coalescence commences at 80 °C and above this temperature C is eluted *after* D (the separation is preferentially entropy-controlled) implying that the stronger complexing enantiomer D is eluted first (!) because of a higher freedom of disorder in the complexed state. The van't Hoff plot depicted in Fig. 24 (bottom) is strictly linear and intersects the line for $-\Delta_{D,L}(\Delta G)=0$ perfectly at the measured value for $T_{isoenant}$ [27]. It is interesting to note that no peak inversion was observed for the enantiomers of the *Z*-diastereomer A and B on **5a** [84] and on **5d** [27].

The inherent principle of enthalpy/entropy compensation in complexation GC was later confirmed with a different selectand, i.e. racemic isopropyloxirane on **5e** (cf. Fig. 26, top) [28,36].

Thus coordination between the (*R*)- and (*S*)-enantiomers of isopropyloxirane and nickel(II)–*bis*[3-(heptafluorobutanoyl)-8-methylene-(1*R*,7*R*)-camphorate] **5e** steadily decreases between 55 and 110 °C as seen from the drop of the retention time from 50 to 2.5 min, respectively (cf. Fig. 26, top). While no separation of the enantiomers is observed between 70 and 90°C, the (*R*)-enantiomer is eluted after the (*S*)-enantiomer at 55°C. Above the coalescence region at $T_{isoenant}$, $-\Delta_{D,L}(\Delta G)$ increases again with a reversal of its sign and enantiomer separation resumes at 110 °C whereby the *S*-enantiomer is now eluted after the *R*-enantiomer (*peak inversion of the second kind*). As expected from the thermodynamic origin of the phenomenon and the validity of Eq. (20), the van't Hoff plot of $-\Delta_{D,L}(\Delta G)/T=R\ \ln(K_D/K_L)$ vs. $1/T$ at five temperatures between 55 and 110 °C is *strictly linear* as evident from Fig. 26, bottom, intersecting the line for $-\Delta_{D,L}(\Delta G)=0$ at the coalescence temperature $T_{isoenant} \sim 89$ °C observed

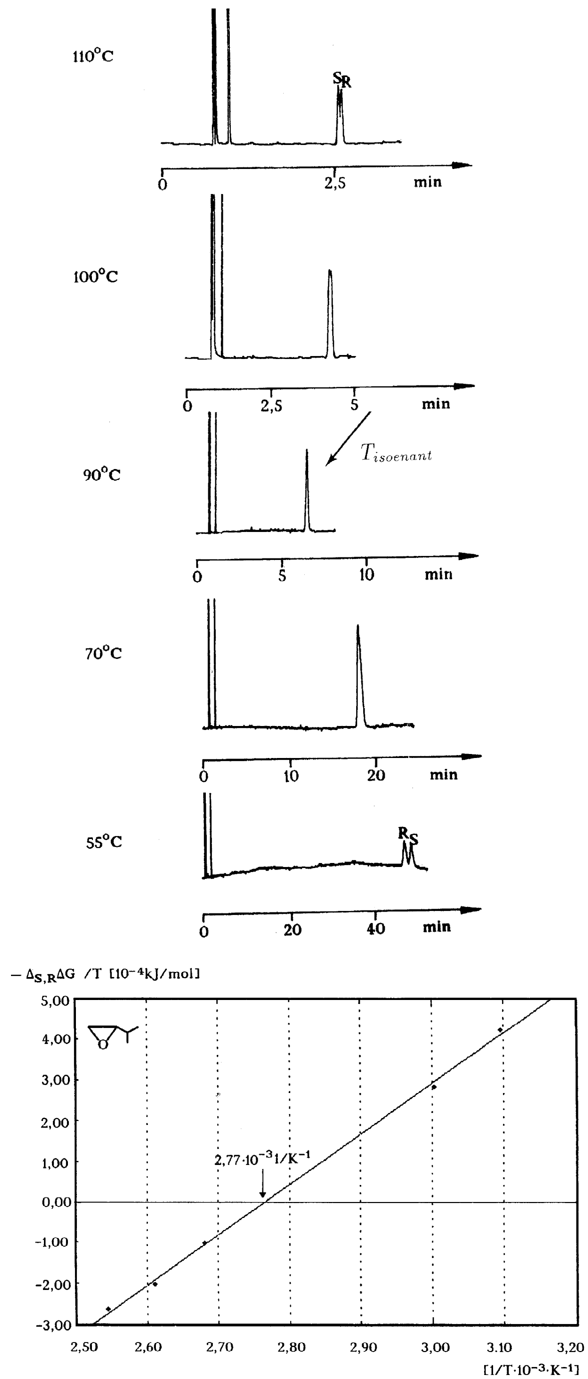

Fig. 26. Top: Temperature-dependent reversal of the elution order of the enantiomers of isopropyloxirane by complexation GC on nickel(II)–*bis*-[3-(heptafluorobutanoyl)-(1*R*)-8-methylene-camphorate] **5e**. Bottom: Linear van't Hoff-plot and determination of the isoenantioselective temperature $T_{isoenant}$ [27,36].

experimentally according to Fig. 26, top (cf. arrow). The van't Hoff plot yields the following thermodynamic data (the subscripts D and L merely denote enantiomers, irrespective of the absolute configuration of isopropyloxirane):

Isopropyloxirane on **5a**:
$-\Delta_{D,L}(\Delta H) = 0.297$ kcal/mol
$\Delta_{D,L}(\Delta S) = -0.82$ cal/K mol
$T_{isoenant} = 362$ K (~89°C)

Quite unexpectedly, minor structural modifications of the selector in a position opposite to the coordination site (at C(8) of camphor) influenced markedly $T_{isoenant}$ for isopropyloxirane (cf. Table 2, left). Also minor changes of the oxirane structure drastically influenced $T_{isoenant}$ (cf. Table 2, right). Thus for the diastereomeric *sec*-butyl-oxiranes only one of the two enantiomeric pairs (*R,S*/*S,R*) showed a low $T_{isoenant}$ similar to that observed for isopropyloxirane whereas for the other pair (*R,R*/*S,S*) $T_{isoenant}$ was more than 500 K (!) higher (cf. Table 2, right) [36].

It should be noted that a low value for $T_{isoenant}$ has only been observed for isopropyloxirane on **4a**, **5a** and **5b** and for one of the diastereomers of *sec*-butyloxirane, but not for other alkylsubstituted oxiranes. Surprisingly, the enantiomers of isopropyloxirane are separated with a separation factor of $\alpha = 1.5$ on **5b** and **5c** at 70 °C (cf. Fig. 3), the temperature where peak coalescence is observed with **4a**, **5a**, **5b**, **5e** and **5f**. The reasons for these unexpected observations are unknown at present. Enantioselective complexation GC involves only a one-point bonding interaction of the solute and the metal center. Enantiorecognition is therefore mainly governed by non-covalent interactions. Although the selector–selectand system in complexation GC is rather simple, involving small chiral molecules such as alkyloxiranes, no mechanistic conclusions have emerged yet, rendering more complicated systems even more difficult to rationalize despite many ambitious efforts reported in the contemporary literature (mainly concerned with LC). Enthalpy/entropy compensation complicates the rationalization of the mechanisms of enantioselectivity. Above $T_{isoenant}$ preferential recognition of one enantiomer is essentially caused by an entropy effect due to a higher degree of disorder of complexation, whereas below $T_{isoenant}$ enantiorecognition is essentially caused by

Table 2
Left: Thermodynamic data of enantioselectivity for isopropyloxirane and structurally modified nickel(II) selectors **4a**, **5e** and **5f**; left: dependence of the structure of the selector; right: dependence of the configuration of the selectands isopropyl- and *sec*-butyloxirane (two enantiomeric pairs) [28,36]

For Isopropyloxirane and Structurally Modified Nickel(II) Selectors					For Isopropyloxirane and *sec*-Butyloxirane **4a**				
		$-\Delta_{S,R}(\Delta H°)$ (cal/mol)	$\Delta_{S,R}(\Delta S°)$ (cal/mol K)	T_{iso} (°C)			$-\Delta_{S,R}(\Delta H°)$ (cal/mol)	$\Delta_{S,R}(\Delta S°)$ (cal/mol K)	T_{iso} (°C)
5e	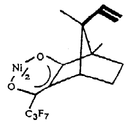	297	− 0,82	89	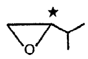		270	− 0,80	64
4a	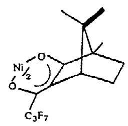	270	− 0,80	64	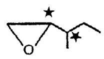	threo	286	− 0,78	94
						erythro	179	− 0,20	622
5f	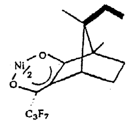	152	− 0,52	19					

the enthalpy effect of chemical bonding. Thus entropic contributions to enantiorecognition represent an important parameter not to be neglected in mechanistic considerations of enantioselectivity (e.g. by molecular modeling studies). Decreasing the temperature below $T_{isoenant}$ as much as possible is always beneficial for chromatographic separation of enantiomers. The separation of enantiomers as determined by $R\ \ln(R'_D/R'_L)$ becomes independent of the temperature when $-\Delta_{D,L}(\Delta H)$ is zero. In this case enantiorecognition is only entropy-controlled. No such an effect has been reported thus far.

An unusual increase of the separation factor α with an increase of the temperature has been observed for the racemic drug mecoprop on Chirasil-Nickel **7a** in complexation SFC that has tentatively been discussed to arise from enthalpy/entropy compensation [59].

2.7. Peak profiles due to enantiomerization – access to kinetic activation parameters of interconversion by peak form analysis

In 1890, Alfred Werner extended the concept of van't Hoff and Le Bel on the tetrahedral tetravalent carbon to pyramidal trivalent nitrogen, however, classical attempts to resolve racemic tertiary amines <u>N</u>XYZ failed (cf. references in [86]). A strategy toward stable stereogenic nitrogen relies on the design of molecular architectures containing nitrogen as a bridge head. Indeed, Prelog and Wieland separated the enantiomers of Tröger's base by liquid chromatography on lactose in 1944 [87]. Another strategy toward an increase of the inversion barrier of pyramidal nitrogen consists of the incorporation of nitrogen in a three-membered ring concomitant with the introduction of lone-pair containing atoms on nitrogen. In 1955 Zlatkis attempted to resolve a chiral aziridine by GC using a chiral stationary phase [88]. This challenge was solved only in 1979 by the separation of 1-chloro-2,2-dimethylaziridine with the large separation factor of $\alpha = 1.43$ using a 100 m× 0.5 mm nickel capillary column coated with optically active nickel(II) *bis*[3-(trifluoroacetyl)-(1*R*)-camphorate] [89]. The separation of the enantiomers could even be performed using a preparative packed column [60] (cf. Section 1.6.). In Ref. [89] it was stated with foresight: *Furthermore, complexation chromatography may develop into a simple method for the investigation of slow inversion processes. If inver-*

sion takes place during the separation process the resulting phenomena of peak coalescence should lend themselves to kinetic analysis.

Indeed a typical peak profile, characterized by the appearance of an overlapping zone called plateau and caused by inverted molecules, was subsequently observed for 1-chloro-2,2-dimethylaziridine by complexation GC on the chiral selector **3a** [20] (cf. Fig. 27, top, left).

The observed peak profile of interconversion was the first such a case reported in chiral chromatography. It represented not only a diagnostic tool for the recognition of inversion of chirality but it was amenable to the acquisition of kinetic data by computerized peak form analysis [90]. Thus by iterative comparison of simulated and experimental chromatograms kinetic data of activation, i.e. the inversion barrier, were obtained [90]. In the follow-

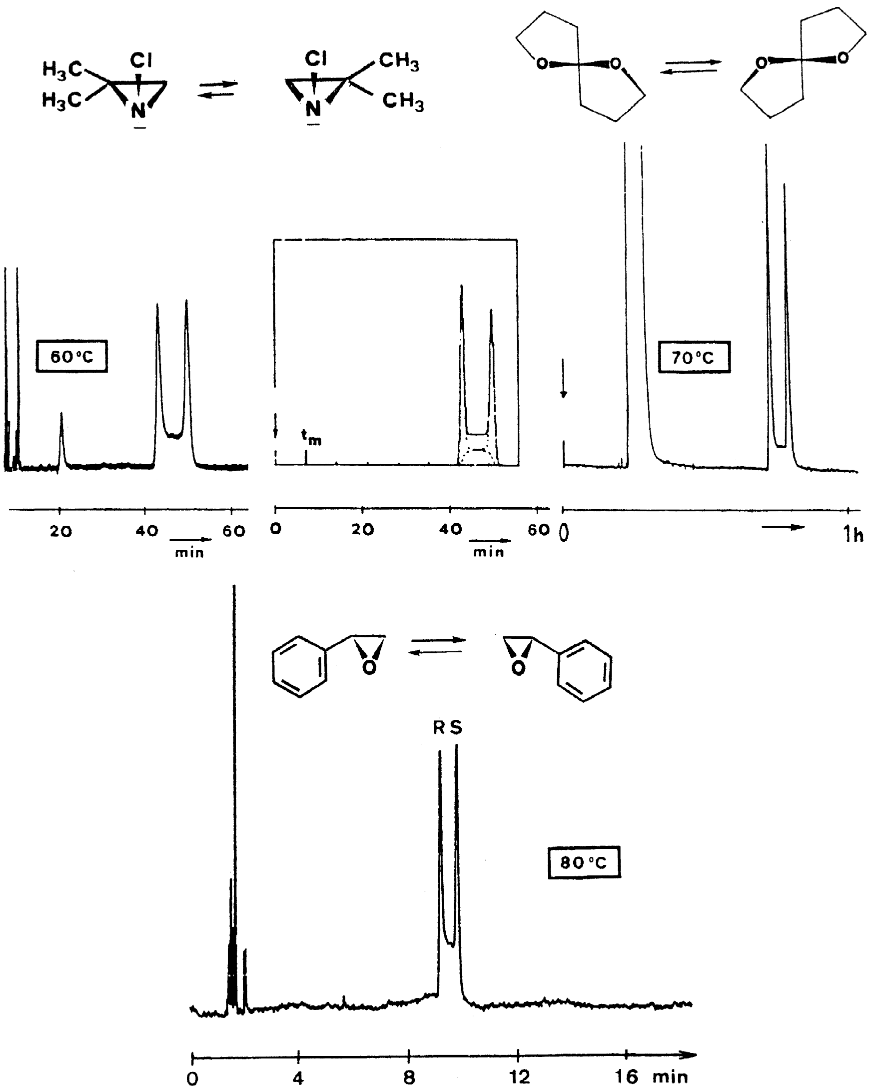

Fig. 27. Plateau-formation due to enantiomerization. Top: peak profiles of interconverting enantiomers during complexation GC of 1-chloro-2,2-dimethylaziridine (left) at 60 °C on **3a** and of 1,6-dioxaspiro[4.4]nonane (right) at 70 °C on **4a** [20]. Left and right: experimental chromatograms. Center: simulated chromatogram [90]. Bottom: peak profile of the enantiomerization of phenyloxirane (styrene oxide) at 80 °C at **4c** [28,36].

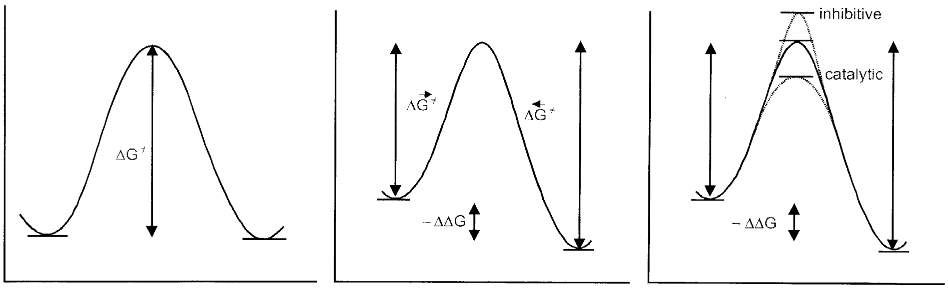

Fig. 28. Kinetic enantiomerization profiles. Left: in the absence of a chiral selector. Center: in the presence of a chiral selector. Right: in the presence of a chiral selector displaying an inhibitive or catalytic effect.

ing years the simulation programs pertinent to complexation GC have steadily been improved using the theoretical plate model and/or the stochastic model, i.e. by the programs SIMUL [91] and CHROMWIN [92,93]. An approximation function for the direct calculation of rate constants and Gibbs activation energies of enantiomerization of racemic mixtures from chromatographic parameters in dynamic chromatography was developed recently [94].

In the References [20,90] the terms *enantiomerization*[12] and *dynamic* were introduced in connection with the chromatography of interconverting molecules. The term enantiomerization implies a process in which the individual stereoisomers of a racemic or enriched mixture of enantiomers undergo inversion of chirality during their chromatographic separation. The equilibrium of enantiomerization, i.e. $L \rightleftharpoons D$, occurs independently in the mobile and stationary phase and is governed only by an entropic change. It represents a simple reversible unimolecular reaction. If enantiomerization is rapid at the chromatographic time scale only one peak will be observed (*peak coalescence of the forth kind*, cf. Section 2.11).

Peak profiles caused by interconversion can be calculated based on the cyclic process, obeying the principle of microscopic reversibility, shown in Scheme 7, top.

The interconverting enantiomers possess a different energy in the chiral stationary phase due to different apparent distribution constants $K_{L(D)} > K_{L(L)}$ (cf. Eq. (7) and Scheme 7, top) that lead to enantiomeric separation. Hence, the interconversion rates

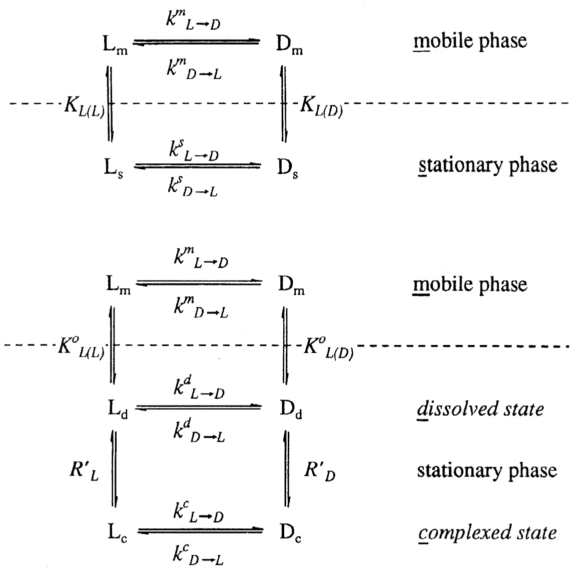

Scheme 7. Top: cyclic process involving enantiomerization in the mobile and the chiral stationary phase [90]. Bottom: cyclic process involving enantiomerization in the mobile and the diluted chiral stationary phase (A in S) [96].

are rendered enantioselective in the environment of the chiral stationary phase (cf. Fig. 28, middle) and $k^s_{L\to D}$ and $k^s_{D\to L}$ are become *different* (cf. Scheme 7) [90].

$$\frac{K_{L(D)}}{K_{L(L)}} = \frac{k^s_{L\to D}}{k^s_{D\to L}} \tag{30}$$

Although the first-eluted enantiomer L is inverted at a higher rate into the second eluted enantiomer D ($k^s_{L\to D} > k^s_{D\to L}$), the former is not depleted but is re-formed due to the longer residence time of the second eluted enantiomer D in the column ($K_{L(D)} >$

[12] Enantiomerization should be distinguished from racemization. The rate laws differ by a factor of 2: $k_{rac} = 2\ k_{enant}$ [95].

$K_{L(L)}$). As a consequence, depletion and enrichment of L (and, *mutatis mutandis*, enrichment and depletion of D) cancel each other and no overall de-racemization is observed. However, de-racemization in favour of the second eluted enantiomer may be predicted when the temperature is raised or the carrier gas flow is enhanced after the first enantiomer is eluted from the column.

A more complicated situation arises when the chiral selector is present in a dissolved state, i.e., A in S. In this case three independent equilibria may be distinguished (cf. Scheme 7, bottom) which are interrelated by the apparent distribution constant K_L according to Eq. (7) and the retention-increment R' according to Eq. (16) [96]. The overall rate constants k^s of interconversion in the stationary phase can be calculated from the rate constants k^d (related to the dissolved state in S) and k^c (related to the complexed state with A in S) by [96]

$$k^s_{L\to D} = \frac{1}{1+R'_L}k^d + \frac{R'_L}{1+R'_L}k^c_1 \tag{31}$$

$$k^s_{D\to L} = \frac{1}{1+R'_D}k^d + \frac{R'_D}{1+R'_D}k^c_{-1} \tag{32}$$

Further examples featuring enantiomerization in complexation GC have been described for 1,6-dioxaspiro[4.4]nonane (cf. Fig. 27, top right) [20], phenyloxirane (cf. Fig. 27, bottom) [36], isopropenyloxirane [36], homofuran (cf. Fig. 29) [97] and the allene dimethyl-2,3-pentadienedioate (cf. Fig. 30) [98]. For homofuran, a perfect agreement between experimental and calculated chromatograms was obtained. Moreover, the enantiomerization barrier calculated by complexation GC corresponded to that measured by polarimetry for an optically enriched sample. Enantiomerization was rapid at the chromatographic time scale at elevated temperature

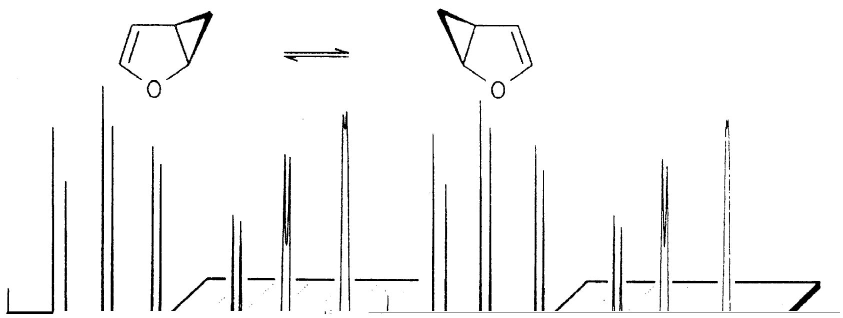

Fig. 29. Comparison of experimental (left) and calculated (right) chromatograms displaying enantiomerization of homofuran by dynamic complexation GC on Chirasil-Nickel **7a**; 10 m×0.1 mm I.D. fused-silica column coated with 0.25 μm **7a** [97].

Temperature-dependent kinetic studies can easily be performed by complexation GC. Thus for the chiral allene dimethyl-2,3-pentadienedioate entropic and enthalpic activation parameters are accessible using the Eyring equation, cf. Fig. 30 (data are given in Ref. [98]).

A very complex interconversion profile has been observed for the epimerization of chalcogran (A⇌D and B⇌C) on Chirasil-Nickel **7a**. The selector is apparently present in a catalytically active state after prolonged time of use (cf. Fig. 31).

The investigations on enantiomerization barriers were recently stimulated by legislative demands. Thus the Federal Drug Administration (FDA) requires that *the stability protocol for enantiomeric drug substances and drug products should include a method or methods capable of assessing the stereochemical integrity of the drug substance and drug product* [93]. Dynamic chromatography and stopped-flow techniques require only minute amounts of the racemic sample rather than isolated enantiomers for the acquisition of inversion barriers [93].

2.8. Kinetic resolution during the separation of enantiomers by complexation GC

The quantitative separation of enantiomers by complexation GC is a useful tool for the precise determination of enantiomeric ratios *er* (cf. (4) in Scheme 5) [64,19]. A serious error in the determination of enantiomeric ratios may be caused by preferential loss of one enantiomer during the gas chromatographic separation process (cf. Section 1.9). Non-enantioselective decomposition of a chiral selectand leads to a preferential depletion of the second eluted enantiomer spending a longer time in the column. Enantioselective decomposition mediated by the chiral metal coordination compound may in principle lead to a depletion of the first or the second eluted enantiomer. Both phenomena have been observed with oxiranes [21,36]. A deviation from the expected 1:1 ratio for racemic *n*-decyloxirane separated at 150 °C on Chirasil-Nickel **7a** and showing an apparent *ee* of 25% is depicted in Fig. 32 [36].

Apart from the preferential depletion of the first eluted enantiomer, a new broad elution zone, probably resulting from an unidentified reaction product,

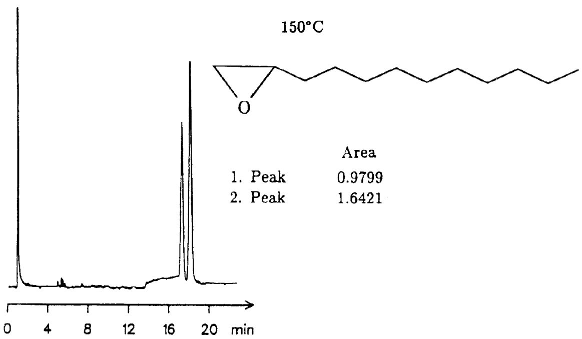

Fig. 32. Deviation from the expected 1:1 ratio (*first* peak diminished) upon enantiomer separation of *racemic* *n*-decyloxirane on Chirasil-Nickel **7a** by complexation GC at 150 °C [36].

occurs. Reversing the chirality of the selector does not alter the observed peak profiles since two enantioselective processes are involved, i.e. chromatographic resolution and kinetic resolution.

2.9. Unusual peak-broadening phenomena in complexation GC

Still another metal-mediated enantioselective phenomenon has been discovered in enantioselective complexation GC involving racemic *trans*-2,3-diethyl-oxirane [36]. As shown in Fig. 33, the first eluted enantiomer shows a considerably broader peak width, also recognized by the reduced peak height, as compared to the second eluted enantiomer although the peak areas are strictly identical. Since in complexation GC peak-broadening is related to the rate of the complexation process, the kinetics of coordination may be different for the two enantiomers. This result could imply that two different coordination sites with different kinetic requirements of the metal(II) selector are involved in the complexation of each individual enantiomer.

A very pronounced broadening of the first peak that occurred only at an intermediate temperature was observed for racemic campher and Chirasil-Nickel **7a** in complexation SFC [57] (cf. Fig. 34). The different approach of the enantiomers of the selectand to opposite sites of a planar coordination geometry of nickel(II) with *cis* configuration has tentatively been proposed [100] (cf. Scheme 8). Another unusual peak broadening phenomenon not yet understood was observed when the enantiomers

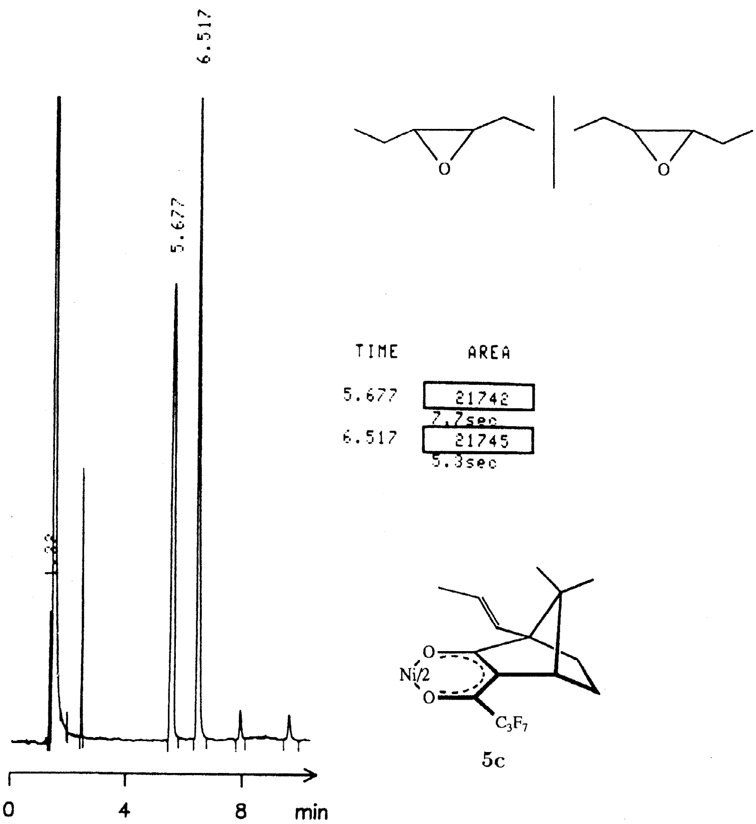

Fig. 33. Deviation from the expected peak width for the first eluted enantiomer of racemic *trans*-2,3-diethyloxirane separated on nickel(II)–*bis*[3-(heptafluorobutanoyl)-10-(ethylidene)-(1*S*)-camphorate] **5c** [36].

of *E*-chalcogran (cf. Scheme 4) were separated on **5a** and underwent coalescence at $T_{isoenant}$ (Note (6) in Ref. [84]).

2.10. The distinction of four enantioselective processes in complexation gas chromatography

Four different enantioselective processes can be discerned in the complexation of *racemic* oxiranes with nickel(II)–*bis*[3-(heptafluoro-butanoyl)-(1*R*)-camphorate] **4a** or derivatives thereof [12]:

- enantioselective coordination (via distinct thermodynamics)
  peak ratio 1:1 (chromatographic separation mediated by the chiral metal selector) cf. Fig. 3
- enantioselective coordination (via distinct thermodynamics and distinct kinetics)
  peak ratio 1:1, unusual peak width (different complexation sites at the metal selector) cf. Fig. 33
- enantioselective enantiomerization
  terminal peak ratio 1:1 and internal plateau formation (different rate of enantiomerization mediated by the chiral metal selector according to Eq. (30)), cf. Fig. 27, bottom
- enantioselective reaction
  peak ratio $\neq$1:1 (kinetic resolution mediated by the chiral metal selector) cf. Fig. 32.

These enantioselective processes are easily detected in the chromatographic complexation column. The observations may guide further investigations in static reaction devices (e.g. kinetic resolution).

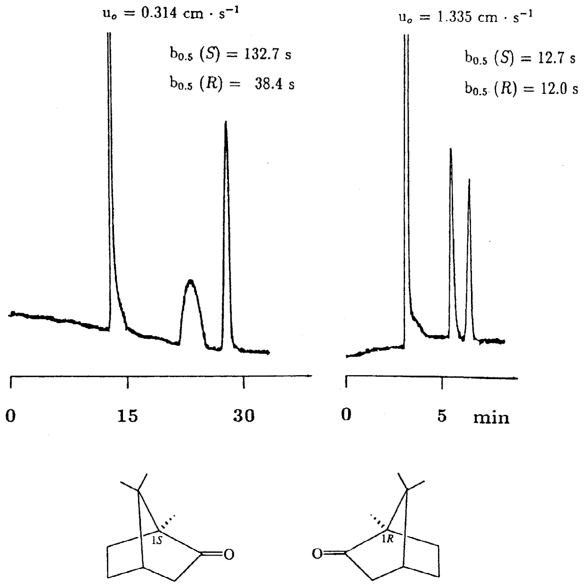

Fig. 34. Peak-broadening phenomenon for the enantiomers of camphor separated on Chirasil-Nickel **7a** by complexation SFC at 60 °C and 15 MPa CO_2 at different flow-rates [100].

2.11. The distinction of four coalescence phenomena in enantioselective complexation gas chromatography

In enantioselective complexation GC four different coalescence phenomena can be distinguished [12]

- peak coalescence (first kind): only one peak is observed due to negligible enantioselectivity of the selector ($-\Delta_{D,L}(\Delta G) < 10$ cal/mol)
- peak coalescence (second kind): only one peak is observed due to a racemic selector
- peak coalescence (third kind): only one peak is observed at the isoenantioselective temperature $T_{isoenant}$ cf. Section 2.6
- peak coalescence (fourth kind): only one peak is observed due to fast enantiomerization of the selectand at the chromatographic time scale cf. Section 2.7.

With chalcogran stereoisomers, the kinetic interconversion and the thermodynamic coalescence phenomenon can be observed at the same time (epimerization of C and D at $T_{isoenant}$ to A and B (cf. Figs. 24 and 31)).

Two further cases of peak coalescence have been detected elsewhere [101]

- peak coalescence (fifth kind): only one peak is observed due to compensation of enantioselectivity of two (or more) competing chiral selectors present in the stationary phase, in the mobile phase, or in both
- peak coalescence (sixth kind): only one peak is observed due to slow instrumental response factors in very fast separations of enantiomers

3. Conclusion

The introduction of chemical selectivity into the gas chromatographic separation process permits the solution of particular difficult separation problems involving isomers, isotopomers and enantiomers. Enantioselective complexation GC represents a mature method capable of solving difficult problems in the analysis of enantiomers. Yet with the introduction of modified cyclodextrins as CSPs in GC in the late 1980s [102,103] its practical importance has diminished. The method however retains its importance in the elucidation of inherent principles of enantioselective chromatography as a whole. Thus in complexation GC, the underlying enantioselective complexation equilibria can easily be quantified. Equations have been developed that permit the calculation of thermodynamic data of molecular association between the selector A and competing selectands B_i in the inert solvent S over a wide temperature range. The concept of the retention-increment (chemical retention factor) R' of B on A, measured from relative retention data r° and r, can be used to quantify enantioselectivities. From the temperature dependence of $-\Delta_{D,L}(\Delta G)$, the Gibbs–Helmholtz parameters $-\Delta_{D,L}(\Delta H)$ and $\Delta_{D,L}(\Delta S)$ determining enantioselectivity $-\Delta_{D,L}(\Delta G)$ are also accessible.

Acknowledgements

The author thanks the late Professor Emanuel Gil-Av for his input and steady interest in the field of complexation GC. He is indebted to his capable coworkers, mentioned in the reference list, for their invaluable contributions to complexation GC. Generous support by the Deutsche Forschungsgemeinschaft and the Fonds der Chemischen Industrie is gratefully acknowledged.

References

[1] E. Gil-Av, B. Feibush, R. Charles-Sigler, Tetrahedron Lett. (1966) 1009.
[2] F. Mikeš, The Resolution of Chiral Compounds by Modern Liquid Chromatography, Thesis, The Weizmann Institute of Science, Rehovot, 1975, p. 1.
[3] V. Schurig, Angew. Chem. Int. Ed. 15 (1976) 304.
[4] B.W. Bradford, D. Harvey, D.E. Chalkley, J. Inst. Petrol., London 41 (1955) 80.
[5] E. Gil-Av, J. Herling, J. Phys. Chem. 66 (1962) 1208.
[6] M.A. Muhs, F.T. Weiss, J. Am. Chem. Soc. 84 (1962) 4697.
[7] R.J. Cvetanovič, F.J. Duncan, W.F. Falconer, R.S. Irwin, J. Am. Chem. Soc. 87 (1965) 1827.
[8] V. Schurig, E. Gil-Av, J. Chem. Soc. Chem. Commun. (1971) 650.
[9] E. Gil-Av, V. Schurig, Anal. Chem. 43 (1971) 2030.
[10] V. Schurig, R.C. Chang, A. Zlatkis, E. Gil-Av, F. Mikeš, Chromatographia 6 (1973) 115.
[11] V. Schurig, Inorg. Chem. 25 (1986) 945.
[12] V. Schurig, Molecular association in complexation GC, in: K. Jinno (Ed.), Chromatographic Separations Based on Molecular Recognition, Wiley–VCH, New York, 1996, Chapter 7, p. 371.
[13] B. Feibush, M.F. Richardson, R.E. Sievers, C.S. Springer Jr., J. Am. Chem. Soc. 94 (1972) 6717.
[14] V. Schurig, Inorg. Chem. 11 (1972) 736.
[15] V. Schurig, Angew. Chem. Int. Ed. 16 (1977) 110.
[16] V. Schurig, E. Gil-Av, Isr. J. Chem. 15 (1976/77) 96.
[17] V. Schurig, Angew. Chem. Int. Ed. 20 (1981) 807.
[18] V. Schurig, Chromatographia 13 (1980) 263.
[19] V. Schurig, in: J.D. Morrison (Ed.), Asymmetric Synthesis, Vol. I, Academic Press, New York, 1983, p. 59.
[20] V. Schurig, W. Bürkle, J. Am. Chem. Soc. 104 (1982) 7573.
[21] V. Schurig, J. Chromatogr. 441 (1988) 135.
[22] V. Schurig, in: P. Schreier (Ed.), Bioflavour '87, de Gruyter, Berlin, 1988, p. 35.
[23] V. Schurig, U. Leyrer, R. Weber, J. High. Resolut. Chromatogr. Chromatogr. Commun. 8 (1985) 459.
[24] V. Schurig, A. Ossig, R. Link, J. High. Resolut. Chromatogr. Chromatogr. Commun. 11 (1988) 89.
[25] R. Weber, V. Schurig, Naturwiss. 71 (1984) 408.
[26] V. Schurig, Angew. Chem. Int. Ed. 23 (1984) 747.
[27] H. Laderer, Thesis, University of Tübingen, 1990.
[28] V. Schurig, D. Wistuba, H. Laderer, F. Betschinger, in: K.H. Dötz, R.W. Hoffmann (Eds.), Organic Synthesis via Organometallics, Vieweg, Braunschweig, 1991, p. 241.
[29] U. Leyrer, Thesis, University of Tübingen, 1985.
[30] B.T. Golding, P.J. Sellars, A.K. Wong, J. Chem. Soc. Chem. Commun. (1977) 570.
[31] V. Schurig, R.C. Chang, A. Zlatkis, B. Feibush, J. Chromatogr. 99 (1974) 147.
[32] V. Schurig, R. Weber, Angew. Chem. Int. Ed. 22 (1983) 772; V. Schurig, R. Weber, Angew. Chem. Suppl. (1983) 1130.
[33] V. Schurig, R. Weber, J. Chromatogr. 289 (1984) 321.
[34] H.B. Kagan, H. Mimoun, C. Mark, V. Schurig, Angew. Chem. Int. Ed. 18 (1979) 485.
[35] V. Schurig, F. Betschinger, Bull. Soc. Chim. Fr. 131 (1994) 555.
[36] V. Schurig, F. Betschinger, Chem. Rev. 92 (1992) 873.
[37] V. Schurig, D. Wistuba, Angew. Chem. Int. Ed. 23 (1984) 796.
[38] D. Wistuba, H.-P. Nowotny, O. Träger, V. Schurig, Chirality 1 (1989) 127.
[39] D. Wistuba, V. Schurig, Chirality 4 (1992) 178 and 185.
[40] D. Wistuba, V. Schurig, Angew. Chem. Int. Ed. 25 (1986) 1032.
[41] B. Koppenhoefer, V. Schurig, Org. Synth. 66 (1987) 160.
[42] V. Schurig, H. Laderer, D. Wistuba, A. Mosandl, V. Schubert, U. Hagenauer-Hener, J. Ess. Oil Res. 1 (1989) 209.
[43] J. Jauch, D. Schmalzing, V. Schurig, R. Emberger, R. Hopp, M. Köpsel, W. Silberzahn, P. Werkhoff, Angew. Chem. Int. Ed. 28 (1989) 1022.
[44] R. Weber, K. Hintzer, V. Schurig, Naturwiss. 67 (1980) 453.
[45] K. Hintzer, R. Weber, V. Schurig, Tetrahedron Lett. 22 (1981) 55.
[46] G. Haniotakis, W. Francke, K. Mori, H. Redlich, V. Schurig, J. Chem. Ecol. 12 (1986) 1559.
[47] W. Francke, W. Schröder, Curr. Org. Chem. 3 (1999) 407.
[48] V. Schurig, R. Weber, G.J. Nicholson, A. Oehlschlager, H. Pierce Jr., A.M. Pierce, J.H. Borden, L. Ryker, Naturwiss. 72 (1985) 92.
[49] V. Schurig, Kontakte (Darmstadt) 1 (1986) 2, and cover page.
[50] H. Frank, G.J. Nicholson, E. Bayer, J. Chromatogr. Sci. 15 (1977) 174.
[51] T. Saeed, P. Sandra, M. Verzele, J. Chromatogr. 186 (1980) 611.
[52] W.A. König, The Practice of Enantiomer Separation by Capillary Gas Chromatography, Hüthig, Heidelberg, 1987.
[53] V. Schurig, R. Link, Chiral Separations, in: D. Stevenson, I.D. Wilson (Eds.), Proceedings of the International Meeting on Chromatography, University of Surrey, Guildford, 3–4 September 1987, Plenum Press, New York and London, 1988, p. 91.
[54] V. Schurig, D. Schmalzing, M. Schleimer, Angew. Chem. Int. Ed. 30 (1991) 987.
[55] F. Keller, H. Weinmann, V. Schurig, Chem. Ber./Recueil 130 (1997) 879.
[56] A. Hierlemann, K. Bodenhöfer, M. Fluck, V. Schurig, W. Göpel, Anal. Chim. Acta 346 (1997) 327.
[57] M. Schleimer, M. Fluck, V. Schurig, Anal. Chem. 66 (1994) 2893.
[58] M. Schleimer, V. Schurig, in: B. Wenclawiak (Ed.), Analysis With Supercritical Fluids: Extraction and Chromatography, Springer Laboratory, Berlin, 1992.
[59] V. Schurig, M. Fluck, J. Biochem. Biophys. Methods 43 (2000) 223.
[60] V. Schurig, U. Leyrer, Tetrahedron Asymm. 1 (1990) 865.

[61] V. Schurig, Naturwiss. 74 (1987) 190.
[62] V. Schurig, D. Wistuba, Angew. Chem. Int. Ed. 22 (1983) 772.
[63] C.J. Reich, G.R. Sullivan, H.S. Mosher, Tetrahedron Lett. 17 (1973) 1505.
[64] V. Schurig, in: Stereoselective Synthesis, Houben-Weyl, Methods of Organic Chemistry, Vol. E 21a, Thieme, Stuttgart, New York, 1995, 147.
[65] V. Schurig, B. Koppenhöfer, W. Bürkle, Angew. Chem. Int. Ed. 17 (1978) 937.
[66] V. Schurig, W. Bürkle, K. Hintzer, R. Weber, J. Chromatogr. 475 (1989) 23.
[67] V. Schurig, Enantiomer 1 (1996) 139.
[68] W.L. Tsai, K. Hermann, E. Hug, B. Rohde, A.S. Dreiding, Helv. Chim. Acta 68 (1985) 2238.
[69] V. Schurig, R. Weber, J. Chromatogr. 217 (1981) 51.
[70] W.H. Pirkle, D.W. House, J.M. Finn, J. Chromatogr. 192 (1980) 143.
[71] S. Allenmark, Chirality 5 (1993) 295.
[72] G. Götmar, T. Fornstedt, G. Guiochon, Chirality 12 (2000) 558.
[73] C.L. de Ligny, J. Chromatogr. 69 (1972) 243.
[74] C.L. de Ligny, T. van't Verlaat, F. Karthaus, J. Chromatogr. 76 (1973) 115.
[75] U. Beitler, B. Feibush, J. Chromatogr. 123 (1976) 149.
[76] J. Noyori, M. Kitamura, Angew. Chem. Int. Ed. 30 (1991) 49.
[77] H.B. Kagan, Synlett, Special issue, 2001, 879.
[78] M. Jung, D. Schmalzing, V. Schurig, J. Chromatogr. 552 (1991) 43.
[79] V. Schurig, M. Juza, J. Chromatogr. A 757 (1997) 119.
[80] I. Špánik, J. Krupčik, V. Schurig, J. Chromatogr. A 843 (1999) 123.
[81] T. Beck, J.-M. Liepe, J. Nandzik, S. Rohn, A. Mosandl, J. High Resol. Chromatogr. 23 (2000) 569.
[82] V. Schurig, J. Coord. Chem. 6 (1976) 63.
[83] B. Koppenhoefer, E. Bayer, Chromatographia 19 (1984) 123.
[84] V. Schurig, J. Ossig, R. Link, Angew. Chem. Int. Ed. 28 (1989) 194.
[85] K. Watabe, R. Charles, E. Gil-Av, Angew. Chem. Int. Ed. 28 (1989) 192.
[86] O. Trapp, V. Schurig, J. Am. Chem. Soc. 122 (2000) 1424.
[87] V. Prelog, P. Wieland, Helv. Chim. Acta 27 (1944) 1127.
[88] A. Zlatkis, J. Chromatogr. Libr. 17 (1979) 473.
[89] V. Schurig, W. Bürkle, A. Zlatkis, C.F. Poole, Naturwiss. 66 (1979) 423.
[90] W. Bürkle, H. Karfunkel, V. Schurig, J. Chromatogr. 288 (1984).
[91] M. Jung, Program Simul. No. 620, Quantum Chemistry Program Exchange, QCPE Bull. 3 (1992) 12.
[92] O. Trapp, V. Schurig, Computers and Chemistry 25 (2001) 187.
[93] O. Trapp, G. Schoetz, V. Schurig, Chirality 13 (2001) 403.
[94] O. Trapp, V. Schurig, J. Chromatogr. A 911 (2001) 167.
[95] M. Reist, B. Testa, P.-A. Carrupt, M. Jung, V. Schurig, Chirality 7 (1995) 396.
[96] M. Jung, V. Schurig, J. Am. Chem. Soc. 114 (1992) 529.
[97] V. Schurig, M. Jung, M. Schleimer, F.-G. Klärner, Chem. Ber. 125 (1992) 1301.
[98] V. Schurig, F. Keller, S. Reich, M. Fluck, Tetrahedron Asymm. 8 (1997) 3475.
[99] S. Reich, O. Trapp, V. Schurig, J. Chromatogr. A 892 (2000) 487.
[100] M. Schleimer, Thesis, University of Tübingen, 1992.
[101] V. Schurig, Chirality 10 (1998) 140.
[102] W.A. König, Enantioselective Gas Chromatography With Modified Cyclodextrins, Hüthig, Heidelberg, 1992.
[103] V. Schurig, H.-P. Nowotny, Angew. Chem. Int. Ed. 29 (1990) 939.